

THESIS

FAILURE MODE ANALYSIS OF A POST-TENSION ANCHORED DAM  
USING LINEAR FINITE ELEMENT ANALYSIS

Submitted by

Aimee Corn

Department of Civil and Environmental Engineering

In partial fulfillment of the requirements

For the Degree of Master of Science

Colorado State University

Fort Collins, Colorado

Fall 2014

Master's Committee:

Advisor: Paul Heyliger

Chris Bareither

Scott Glick

Guy Lund

Copyright by Aimee Corn  
All Rights Reserved

## ABSTRACT

### FAILURE MODE ANALYSIS OF A POST-TENSION ANCHORED DAM USING LINEAR FINITE ELEMENT ANALYSIS

There are currently over 84,000 dams in the United States, and the average age of those dams is 52 years. Concrete gravity dams are the second most common dam type, with more than 3,000 in the United States. Current engineering technology and technical understanding of hydrologic and seismic events has resulted in significant increases to the required design loads for most dams; therefore, many older dams do not have adequate safety for extreme loading events. Concrete gravity dams designed and constructed in the early 20<sup>th</sup> century did not consider uplift pressures beneath the dam, which reduces the effective weight of the structure.

One method that has been used to enhance the stability of older concrete gravity dams includes the post-tension anchor (PTA) system. Post-tensioning infers modifying cured concrete and using self-equilibrating elements to increase the weight of the section, which provides added stability. There is a lack of historical evidence regarding the potential failure mechanisms for PTA concrete gravity dams. Of particular interest, is how these systems behave during large seismic events. The objective of this thesis is to develop a method by which the potential failure modes during a seismic event for a PTA dam can be evaluated using the linear elastic finite element method of analysis.

The most likely potential failure modes (PFM) for PTA designs are due to tensile failure and shear failure. A numerical model of a hypothetical project was developed to simulate PTAs in the dam. The model was subjected to acceleration time-history motions that simulated the

seismic loads. The results were used to evaluate the likelihood of tendon failure due to both tension and shear. The results from the analysis indicated that the PTA load increased during the seismic event; however, the peak load in the tendons was less than the gross ultimate tensile strength (GUTS) and would not be expected to result in tensile failure at the assumed project. The analysis also indicated there was a potential for permanent horizontal displacement along the dam/foundation interface. The horizontal movement was not considered large enough to develop a shear failure of the tendons at the project.

The results from this study indicate demand to capacity ratios (DCR) of 0.79 for the anchor head, 0.75 for the tendon, and 0.63 for the foundation cone failure, and a potential displacement of 0.33 inches, which is not large enough to shear the tendon. The methods developed are appropriate for the evaluation of the tensile and shear failure modes for the PTA tendons. Based on the results, it would appear that shear failure of the tendon is a more likely failure mechanism. Thus, shear failure of the tendon should be a focus of seismic evaluations.

## TABLE OF CONTENTS

LIST OF TABLES .....	vi
LIST OF FIGURES .....	vii
CHAPTER 1 : INTRODUCTION .....	1
CHAPTER 2 : LITERATURE REVIEW .....	9
CHAPTER 3 : THE GENERAL DAM .....	18
Concrete Properties .....	20
Foundation Properties .....	24
Forces on the Dam .....	24
Hydrostatic Pressure .....	25
Internal Hydrostatic Pressure (Uplift).....	26
Earthquake .....	27
Loading Combinations.....	28
Load Case I – Usual Load Combination.....	29
Load Case II – Unusual Load Combination .....	29
Load Case III – Extreme Load Combination.....	29
Load Case IV – Post-Earthquake.....	29
Methods of Analysis .....	29
Gravity Method of Analysis.....	30
Finite Element Modeling .....	30
CHAPTER 4 : METHODS OF FAILURE.....	32
The Potential Failure Modes of the Dam.....	32
Concrete Overstressing .....	33
Moment Equilibrium.....	36
Sliding Stability .....	37
Post-Tension Anchor Failure Modes .....	38
Tensile Failure .....	39
Tendon Shear Failure .....	44
CHAPTER 5 : ANALYSIS .....	46

Modeling .....	46
Anchor Design .....	48
Anchor Modeling .....	48
Model Verification .....	51
CHAPTER 6 : RESULTS .....	60
Dam Failure Modes .....	60
Tendon Tensile Failure .....	62
Tendon Shear Failure .....	64
CHAPTER 7 : SUMMARY AND CONCLUSIONS .....	66
BIBLIOGRAPHY .....	69

## LIST OF TABLES

Table 3-1 Summary of Average Concrete Properties from the Design of Small Dams (U.S. Department of the Interior, Bureau of Reclamation, 1987) .....	23
Table 3-2 General Dam Concrete Properties (URS Corp, 2004).....	23
Table 3-3 Foundation Properties (URS Corp, 2004) .....	24
Table 4-1 Allowable Concrete Compressive and Tensile Stress (U.S. Army Corps of Engineers, 1995) .....	35
Table 4-2 Summary of Overturning Criteria Based on the U.S. Army Corp of Engineers (U.S. Army Corps of Engineers, 1995).....	36
Table 4-3 Summary of Minimum Allowable Sliding Factors of Safety based on FERC Guidelines (No Cohesion Assumption) (FERC Guidelines & Federal Energy Regulatory Commission, 1999) .....	37
Table 5-1 Frequency and Spectral Values used for Response Spectra Analysis .....	53
Table 6-1 Preliminary Sliding Stability Factors and Resultant Location .....	61

## LIST OF FIGURES

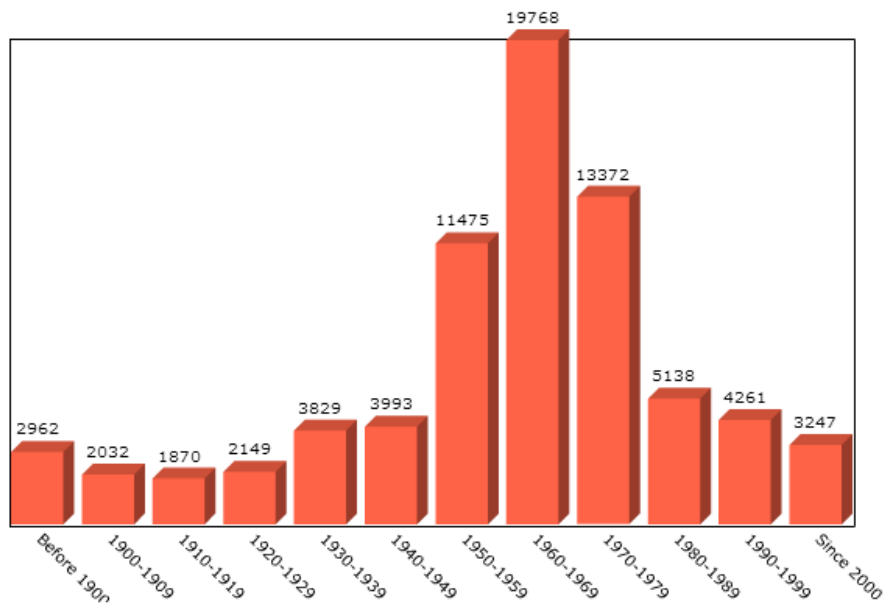
Figure 1-1 Dams by Completion Date (U.S. Army Corps of Engineers) .....	1
Figure 1-2 Dams by Primary Type (U.S. Army Corps of Engineers) .....	2
Figure 1-3 Histogram of Dams Anchored by Year (1962-2004) (Heslin, Bruce, Littlejohn, & Westover, 2009) .....	4
Figure 1-4 Failure Mechanisms of a Post-Tension Anchored Gravity Dam: (a) Example of Post-Tensioning; (b) Possible Dynamic Response; (c) Unbonded Cable Failure Mechanisms at Weak Joints (Morin, Léger, & Tinawi, 2002) .....	6
Figure 1-5 Cable Failure Mechanisms: (a) Tension Failure; (b) Shear-Tension Failure; (c) Shear Failure (Morin, Léger, & Tinawi, 2002) .....	7
Figure 2-1 Plan View of Stewart Mountain Dam (U.S. Department of the Interior, Water and Power Resources Service, 1981) .....	13
Figure 3-1 General Dam Cross Section .....	19
Figure 3-2 Instantaneous and Sustained Modulus of Elasticity of Concrete – Canyon Ferry Dam (U.S. Department of the Interior, Bureau of Reclamation, 1958) .....	22
Figure 4-1 Geometry of Rock Mass Assumed to be Mobilized at Failure (a) Individual Anchor in Isotropic Medium and (b) Line of Anchors in Isotropic Medium (U.S. Army Corps of Engineers, 1994) .....	41
Figure 5-1 Modeled Dam and Foundation .....	47
Figure 5-2 Modeled Dam and Foundation with Link Element .....	50
Figure 5-3 Stress Plots of Static Analysis from Gravity Method of Analysis .....	52
Figure 5-4 Stress Plots of Static Analysis from Finite Element Analysis .....	52
Figure 5-5 First Six Mode Shapes with Post-Tension Anchors from ANSYS .....	54
Figure 5-6 Stress Plots of Pseudo Dynamic Hand Calculations .....	56
Figure 5-7 Stress Plots of Site Specific Finite Element Analysis Response Spectra .....	56
Figure 5-8 Horizontal Time History of 10,000 Year Return Period for Controlling Seismic Event – San Fernando .....	58
Figure 5-9 Stress Plots of Spectrally Scaled Time History Analysis at Time 9.79 sec .....	59

Figure 6-1 Stress Plots of Governing Spectrally Scaled Time History Analysis at Time 1.61 sec  
..... 62

Figure 6-2 Percent Gross Ultimate Tensile Strength of Post-Tension Anchor for Governing Time  
History..... 63

## CHAPTER 1 : INTRODUCTION

There are currently over 84,000 dams in the United States, and the average age of those dams is 52 years. It is estimated that by 2020, 70% of U.S. dams will be more than 50 years old. Figure 1-1 shows the age distribution of the dams in the United States. Older dams were designed and constructed using the standards of practice of the time; however, there have been significant changes in current engineering understanding and the technology used to investigate behavior. As a result, the estimated design loads have increased from the previous standards of practice, and many older dams do not have adequate safety for these extreme loading events. In the 2013 American Society of Civil Engineering (ASCE) Report Card, Dams received a grade of a D, with more than 4,000 dams determined to be deficient (American Society of Civil Engineers, 2013).



**Figure 1-1 Dams by Completion Date (U.S. Army Corps of Engineers)**

A concrete gravity dam is defined by the United States Bureau of Reclamation (USBR) as being: “proportioned so that its own weight provides the major resistance to the forces exerted

upon it... Properly designed and constructed, it will be a permanent structure that requires little maintenance” (U.S. Department of the Interior, Bureau of Reclamation, 1987). According to the U.S. Army Corps of Engineers (USACE), while earth dams make up almost 86% of all dams, concrete gravity dams are the second most common dam type, with approximately 3,000 across the country. The breakdown of dam types in the U.S. is shown in Figure 1-2.

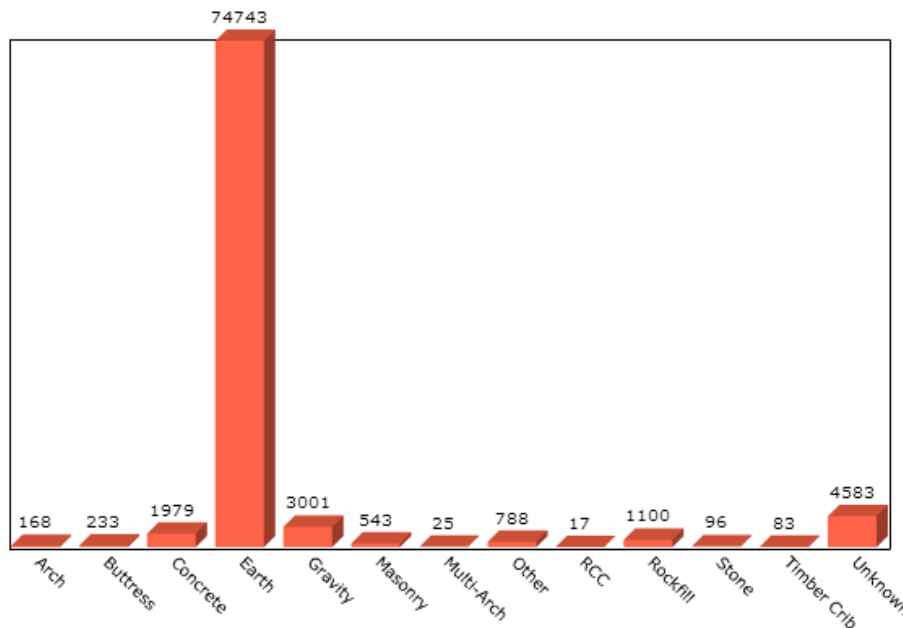


**Figure 1-2 Dams by Primary Type (U.S. Army Corps of Engineers)**

Dams are classified according to their potential risk to property damage, expected life loss, and economic impact, if failure were to develop. Many dams were designed based on a low hazard classification, “a dam located in a rural or agricultural area where failure would only cause the loss of the dam itself but may cause minor damage to nonresidential and normally unoccupied buildings, or rural or agricultural land” (American Society of Civil Engineers, 2013). With an increasing population, by 2050 many dams originally designed as low hazard structures may be re-categorized as significant hazard, “a dam in which the failure or misoperation is not expected to cause loss of life, but results in downstream property, critical infrastructure,

environmental damage, or disruption of lifeline facilities” (American Society of Civil Engineers, 2013). Similarly, the number of high hazard dams, “a dam in which failure or misoperation is expected to result in loss of life and may also cause significant economic losses, including damages to downstream property or critical infrastructure, environmental damage, or disruption of lifeline facilities” is on the rise. In 2012, approximately 14,000 of the over 84,000 dams in the U.S. were classified as high hazard dams (American Society of Civil Engineers, 2013).

Early 20<sup>th</sup> century concrete gravity dams were designed without consideration of internal hydrostatic pressure, also called uplift, a significant load that reduces the effective weight of the structure (i.e. buoyancy) and thus, reduces the safety. Also, better understanding of hydrologic precipitation and seismic events has resulted in significantly higher design loads for these structures. When analysis shows a deficiency in safety, a retrofit of the dam is typically required to increase the capacity for large loads. Post-tensioning of dams is becoming an important method to modify deficient dams due to either larger loads, changing hazard classification, or more stringent safety standards (Morin, Léger, & Tinawi, 2002).

Post-tensioning infers modifying cured concrete and using self-equilibrating elements to effectively increase the weight of the section. This method can be used to increase stability and control over failure mechanisms such as cracking, overturning and sliding. Despite their appeal there is a lack of historical evidence regarding the potential failure mechanisms of post-tensioned concrete gravity dams, primarily because the loads used for design are very infrequent events.

The use of post-tensioned anchors (PTA) has been considered a standard of practice for over 40 years. In 1974, tentative recommendations of practice for pre-stressed rock and soil anchors were issued by the Post-Tensioning Division of the Prestressed Concrete Institute (PCI). Two years later, in 1976 the Post-Tensioning Institute was formed as an independent

organization. *The First Edition of Recommendations for Prestressed Rock and Soil Anchors* were adopted and reprinted by the USACE in 1980 (Heslin, Bruce, Littlejohn, & Westover, 2009).

The first installations of PTAs in Dams, is believed to have occurred in the early 1960s. The histogram shown in Figure 1-3 illustrates the increasing application of PTA tendons in the U.S. To date, the capacity of approximately 400 concrete gravity dams has been increased using PTAs. Two of the first dams to be post-tensioned include John Hollis Bankhead Lock & Dam in Alabama in 1965 and Little Goose Lock & Dam in Washington in 1968.

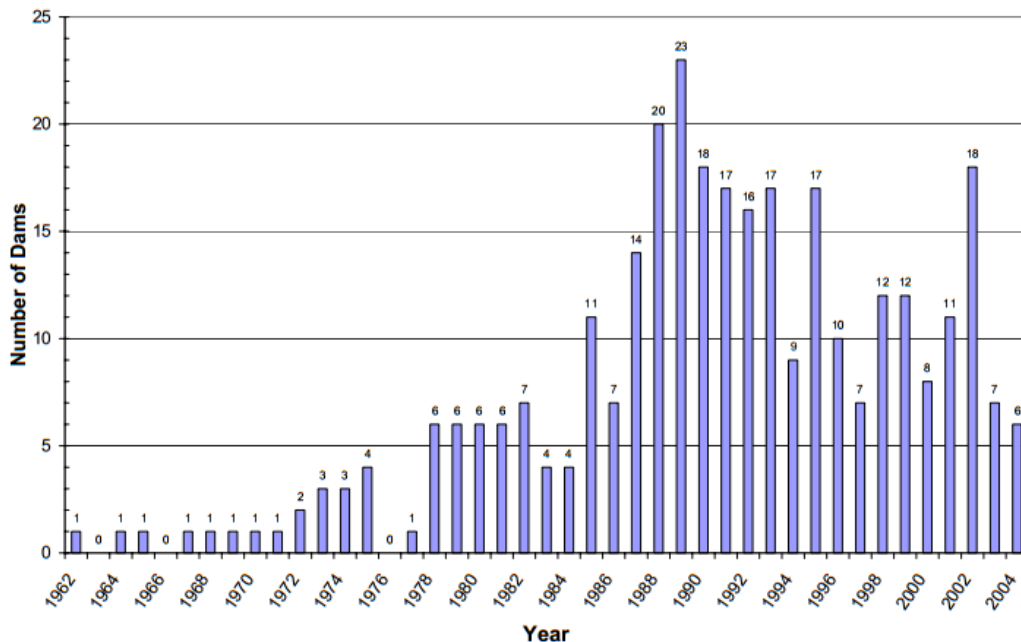


**Figure 1-3 Histogram of Dams Anchored by Year (1962-2004) (Heslin, Bruce, Littlejohn, & Westover, 2009)**

PTAs designed for the probable maximum flood (PMF) or maximum credible earthquake (MCE) are placed near the upstream face and anchored to the foundation. The most popular method to post-tension concrete dams consists of high strength steel and either solid anchor bars or wire cables (tendons). Analysis of potential failure modes of tendons is the focus of this thesis.

PTA tendons can be installed either as bonded or unbonded. A bonded tendon refers to the method in which the free-stress length of the tendon is bonded with the surrounding cement

grout. An unbonded tendon, the focus of this thesis, refers to the method in which the free stress length of the tendon is free to move preventing the tendon/grout interface from developing shear strength. To prevent bond along the free-stress length the tendon is typically coated with grease and encapsulated in plastic sheathing. The load from the unbonded PTA is transferred over a length through shear transfer at the bond interface in the foundation. Unbonded strands have an advantage in that long-term anchor forces can be monitored and cables can be retensioned at a specific capacity to compensate for unforeseen losses.

The behavior of a concrete dam during a seismic event includes oscillation, which can cause potential displacement, and sliding. Oscillation, also called rocking, develops due to the induced ground motions. Oscillations can cause elongation of the tendons resulting in an increase in load, which could cause the load on the tendons to encroach on the guaranteed ultimate tensile strength (GUTS). Sliding can develop if the combined effect of the static and inertia loads exceed the shear capacity along a weak plane within the concrete dam, at the dam/foundation interface, or a discontinuity within the foundation rock. Typically, there are four potential cable failure mechanisms, tensile failure, cable-concrete contact failure, tensile-shear failure, and direct shear failure. Shown below in Figure 1-4 are anticipated failure mechanisms of a post-tensioned anchored dam (Morin, Léger, & Tinawi, 2002).

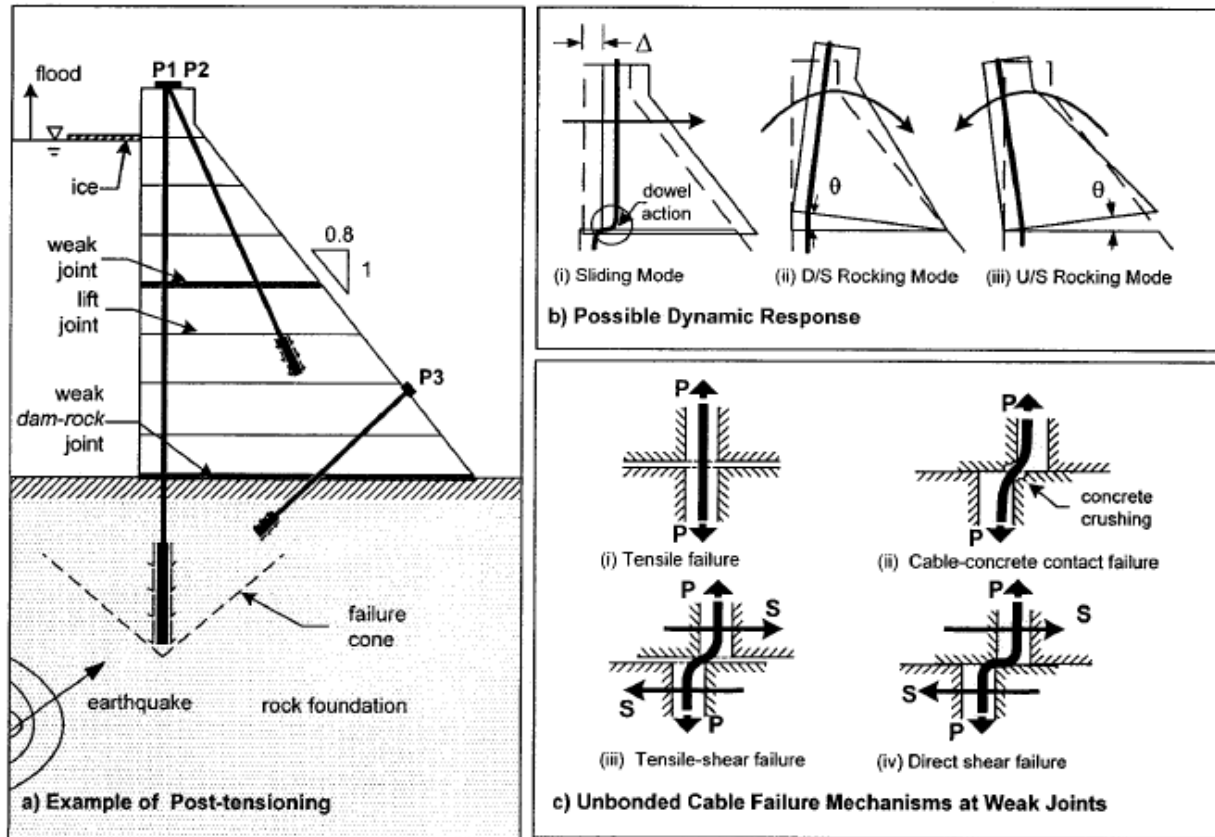


**Figure 1-4 Failure Mechanisms of a Post-Tension Anchored Gravity Dam: (a) Example of Post-Tensioning; (b) Possible Dynamic Response; (c) Unbonded Cable Failure Mechanisms at Weak Joints (Morin, Léger, & Tinawi, 2002)**

Visuals of the cables after failure for tension failure, shear-tension failure, and shear failure are shown in Figure 1-5. Léger and Mahyari, and Hall et al. (as cited in Morin et al., 2002) use a simple uniaxial elastic representation of cables for their finite element models for cracking, sliding, and rocking responses of post-tensioned anchors. Morin et al. states there is little knowledge of the seismic behavior of post-tensioned gravity dams up to time of failure, with no shake table tests to provide experimental evidence to verify the seismic behavior.

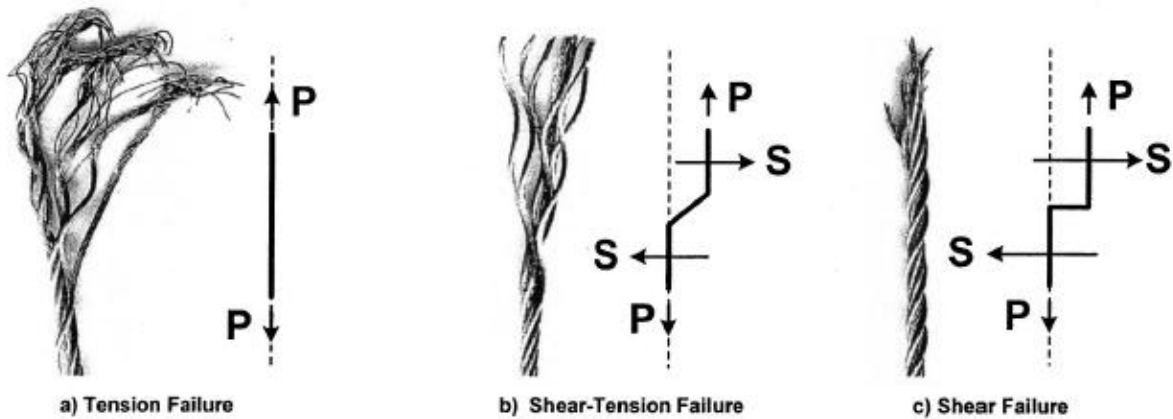


**Figure 1-5 Cable Failure Mechanisms: (a) Tension Failure; (b) Shear-Tension Failure; (c) Shear Failure (Morin, Léger, & Tinawi, 2002)**

Conventional post-tensioned cable design does not consider an increase in tendon force due to shear displacement response, as a function of the residual friction angle and the dilation angle. This results in normal displacement that is strongly related to joint roughness. This is known as the dilatancy phenomenon (Morin, Léger, & Tinawi, 2002). Corns (as cited in Morin et al., 2002) proposed measuring the effectiveness of cables by a force higher than their initial post-tensioned force for grouted-bonded tendons.

The shear strength in the rock mass and along the interface directly depends on confining stresses. PTAs increase confining stress which in turn increases shear strength. A small change in shear capacity can result in large displacements. This becomes a huge concern since the loss of the anchors reduces the confining stress decreasing the shear strength which could lead to a brittle failure of the dam. A brittle failure of a dam is considered to be catastrophic because failure is immediate. Post-tensioning also increases the confining stress across sliding joints, increasing shear resistance. As shown by the experimental work of Cong and Soong Lood (as cited in Morin et al., 2002), anchored blocks were found to be sturdier than free standing ones. Therefore, the PTA tendons also increase the critical acceleration required to initiate sliding.

Given the potential modes of failure for this class of structure, there is a lack of information to adequately analyze the potential failure modes of a post-tension anchored dam. The objectives of this thesis are to develop a method by which the potential failure modes during a seismic event for a post-tension anchored dam can be evaluated using the linear elastic finite element method of analysis. In the remainder of this thesis, the pertinent literature is reviewed, the applicable loads and failure modes are discussed, as well as the finite element model process described and results are presented. Finally, conclusions and recommendations for future work are presented.

## CHAPTER 2 : LITERATURE REVIEW

There are several components to consider as part of this research, each of which has a fairly extensive scientific background. In this chapter, the application in current practice of these components is reviewed and their maturity as an area of research is discussed.

The behavior of post-tension anchor (PTA) tendons relies on several key components, such as the bond strength between the tendon and grout, rate of creep and relaxation after the tendon is locked off.

One of the critical loads that concrete dams must safely withstand is the added forces due to earthquake ground motions. PTAs have been used in several projects to increase the capacity for seismic loads, and Zhang and Ohmachi (1999) have examined the seismic strengthening of many concrete gravity dams with PTAs. The post-tensioned anchor applies a load on the dam which increases the compressive stresses in the concrete which help to offset the development of tensile stress during the earthquake load. The oscillation of the dam due to the earthquake motions results in the development of flexural loads on the dam, and can develop tensile stresses on the face of the structure. If the tensile stress is greater than the tensile strength of the concrete, then the mass concrete can crack which is sometimes called an overstressing failure mechanism.

Concrete cracks that develop due to the seismic loads do not imply failure of the structure. A cracked section does represent a defect within the structure that can alter the capacity of the section (i.e. reduced section modulus). If the load demand from the earthquake is greater than the effective capacity, then a structural failure can develop. Therefore, the potential for cracks to develop within the mass concrete are an important characteristic in the safety evaluation of the structure.

The hydrostatic pressures on the upstream face of the dam along with the seismic loads develop flexural loads on the dam. The weight of the dam causes an axial load on the section of the dam. The flexural and axial loads are distributed across the section of the dam through vertical stresses. If the flexural load is large enough, then vertical tensile stresses can develop at the upstream face of the dam. PTAs are typically arranged in the vertical direction, and increase the axial load on the section, which reduces the potential for tensile stress development on the upstream face.

If the load from the PTA is large enough a localized compressive failure at the anchor head can result. For example, if the force from the PTA tendons is large enough it can induce excessive compressive stress on the concrete, which fails due to the effects from Poisson's ratio (i.e. splitting tensile test for concrete samples).

The research by Zhang and Tatsuo (1999) has shown that post-tension anchors can be used to successfully remediate a concrete gravity dam effectively. However, as stated, the PTAs must be adequately designed. (Zhang & Ohmachi, 1999)

Current design and construction practices typically require the PTAs be embedded in cement grout or grease to protect them from weather elements. Most projects do not have a means in which to test the long-term load after construction is complete. Thus, one question regarding the long-term performance is related to the creep and relaxation that may develop in the post-tension anchor system.

At Highgate Falls Dam in Vermont, a method was developed in which the anchor load could be tested over a long period of time using vibrating wire load cells, as summarized by Mukherjee et al (1999). The measurement from the load cells indicated the anchor load fluctuated, and the load fluctuations correlated to the change in seasonal temperatures. The

maximum load from the PTAs were found to occur at a specific period of time (approximately 2 weeks) after the peak seasonal air temperatures. Temperature loads and thermal characteristics of the concrete dam cause the concrete to expand and contract, which elongates the tendon causing an increase in load.

The measurements also indicate the load from the PTA reduced with time. The decremental trend in the load was not due to debonding at the anchor/grout interface, but rather due to the relaxation and creep of the anchor system (Mukherjee, Lague, Mosher, & Simon, Ph.D., P.E., 1999). Although changes in loading from thermal affects are important in tendon design, it would not cause a tensile failure and is therefore not addressed in this thesis.

One concern with PTAs is the susceptibility to weathering element and therefore, corrosion protection is an important part of the anchor design. Different types of corrosion protection systems have been used in the past. Epoxy coated anchor cables have been used to enhance the protection against corrosion. The effect of epoxy coating must be taken into account in the anchor design.

Studies by Leamon and Dunlap (1994) on Martin Dam evaluated the effectiveness of epoxy coated PTA tendons. Martin Dam is a concrete gravity dam and hydroelectric facility owned by the Alabama Power Company. The tendon design included 63 tendons with 47 in the spillway and 16 in the west non-overflow section. A total of 33 tendons have an anchorage length of 25.5 ft and 14 tendons have an anchorage length of 17 feet. The tendons are all bonded tendons. The design load is 60% guaranteed ultimate tensile strength (GUTS) and were locked off at 70% GUTS. This approximate 10% difference is to account for creep and relaxation of the tendons. Test anchors were stressed to failure of the grout to rock bond to get a reliable strength.

Performance and proof tests were performed on all tendons in accordance with recommendations contained in the Post-Tensioning manual (as cited in Leamon and Dunlap, 1994). Liftoff tests were performed after the tendon was locked off at 80% GUTS. The measured load relaxation was measured over a specified period of time. Based on this data, the epoxy-coated strands may exhibit higher creep and different behavior than what is typical of bare strands. (Leamon & Dunlap, P.E., 1994). Creep and relaxation of the tendons is accounted for in the adjustment between lock-off and design load, and is therefore automatically accounted for in the design of the tendons.

An evaluation of Stewart Mountain Dam in Arizona found that the capacity of the structure was inadequate for the required earthquake magnitude. Post-tension anchors were designed and constructed to remediate the dam for the seismic loads. Bruce and Groneck (1994) examined the dam repair of Stewart Mountain Dam.

Stewart Mountain Dam is a thin-arch dam with two concrete thrust blocks, three concrete gravity sections and a service spillway, as shown in Figure 2-1. The post-tension anchor design included 62 tendons at approximately 8 foot center along the crest. The free lengths varied over 22 feet, with bond lengths ranging from 10-46 feet. The orientation of the tendons varied from vertical to an upstream dip of 8 degrees. The majority of anchors were extended into the bedrock. One-third (22) of the tendons were bonded, epoxy coated strands, for corrosion protection. The design working load was set equal to approximately 50% of GUTS, which averaged 630 kips. Six full scale test anchors confirmed earlier estimates of load transfer between the cable and grout. Grouting was performed in two stages. The tendons were loaded 14 days after grouting, which allowed time for the grout to gain strength and cure. Cyclic performance tests, guided by the post-tensioning institute (as cited by Bruce & Groneck, 1994), were performed. The anchors

were monitored for 100 days for creep and relaxation before they were finally locked off at a minimum 108.5% working load (approximately 55% of GUTS). After the tendon was locked off the tendon free length was tremie grouted with non-shrink grout, to provide an extra layer of corrosion protection and to structurally bond the stressed tendon to the surrounding concrete (Bruce & Groneck, P.E., 1994).

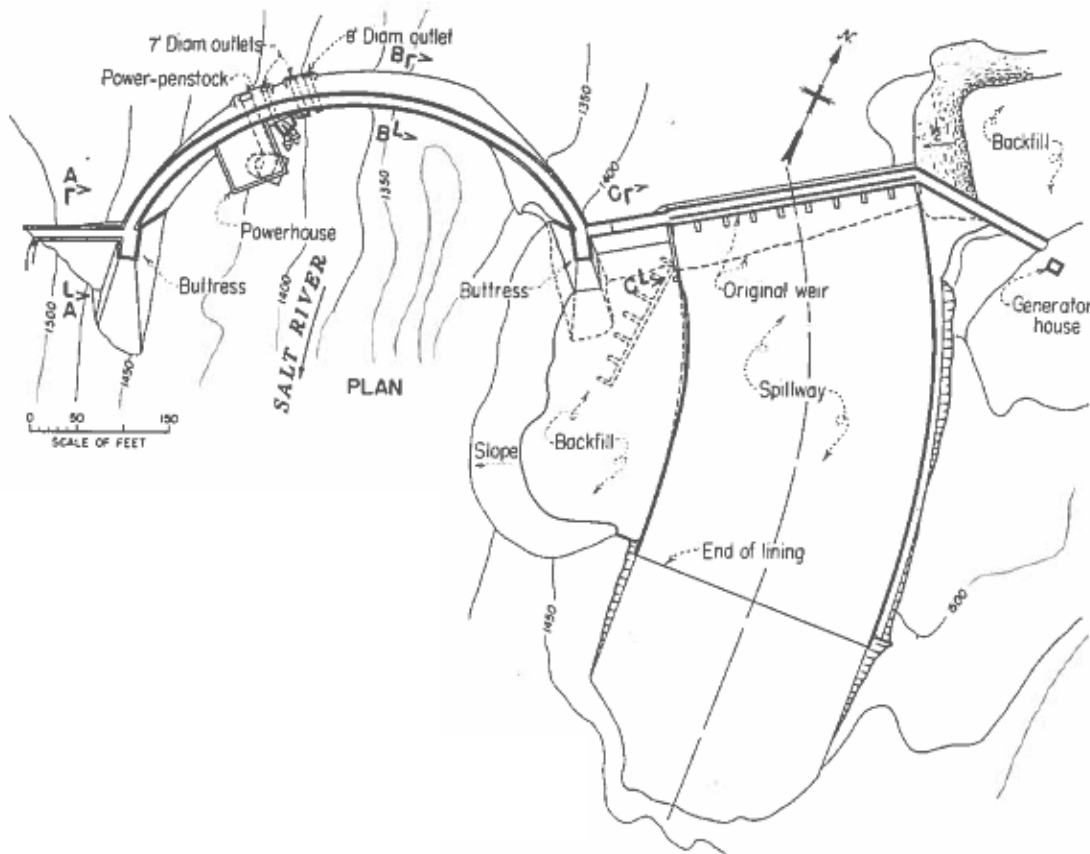


**Figure 2-1 Plan View of Stewart Mountain Dam (U.S. Department of the Interior, Water and Power Resources Service, 1981)**

This article points out the importance of understanding the seismic behavior of a post-tension anchored dam. Understanding of the behavior prevents the use of a 55% GUTS lock-off load, making them more economical.

According to Tinawi et al, 2000 seismic safety is a major concern for concrete dams today, because dams were built many years ago with little consideration for seismic loads. Since their construction, structural dynamics and seismicity has continued to progress. Guidelines currently recommend a high hazard structure meet safety factors for a seismic event with a 3,000 to 10,000 year return period. A 10,000 year return period is used for analysis in this thesis. (Tinawi, Léger, Leclerc, & Cipolla, 2000)

Post-tension anchors are a complex structural system, and require careful adherence to the design specification during construction. This case history example illustrates what can happen if the construction process is performed poorly.

Mortensen et al., 2012 focus on the third post-tensioned anchors installed at Olmos Dam, which gives an excellent example regarding contractor experience and quality control during construction. Olmos Dam is a concrete gravity dam built in 1929. Post-tension anchors were installed in 1974 to provide provided additional safety for hydrologic load due to overtopping and due to the probable maximum flood (PMF). Three of the five anchors failed within the bond zone due to poor grouting. One anchor was broken because of inadequate quality assurance during construction of the anchor couplings. A third anchor failure due to concrete crushing beneath the anchor bearing plate, due to poor concrete consolidation. A failure investigation was done after the first problem in 1984. There was a large spall over the post-tensioned anchor in the downstream face. The investigation began in 1992 after a cap over one anchor was cracked and displaced. Lift-off tests were conducted and the results are of more broad interest than some of the other studies summarized in this chapter. Mortensen and co-workers showed that:

- 9 broken bars – 2 failing in coupling
- 2 deficient bond zones
- 1 bar broken during test
- 1 de-stressed anchor with untightened nut
- 2 bars giving erratic elongation during stressing

The anchors had originally been designed for a design load equal to 44% GUTS so that they could be stressed to a higher load if more existing bar anchors were reported unserviceable. It was recommended to monitor the anchors every five years. The inspection in 2006 revealed the following:

- 3 new broken bars
- 2 bars still damaged
- 1 bar broken during testing
- Continued loss of loads
- Load reduction due to creep or relaxation of approximately 0.3% - 2.7% per year

A study was completed in 2007 to stabilize the dam for a third time. In 2010 and 2011, 68 multi-strand anchors were installed along with piezometers to monitor uplift assumptions, extensometers, and load cells to monitor anchor performance. The design of the new anchor system was conducted in 2009. Fourteen strands at 0.6” diameter of 270 ksi low relaxation uncoated seven wire strands were used with an ultimate bond strength of 218 psi. The highest level of corrosion protection was used. This includes:

- 60 mil high density polyethylene corrugated sheath
- Full free length protected by grease filled polyethylene tubing
- Anchor was fully grouted inside and outside the sheathing
- Head assembly encapsulated beneath grease filled galvanized steel cover with rubber gaskets

During construction, the corrugated sheathing was tested for leaks before and after instillation in the drill hole. The static water level was approximately 50 feet below the top of the dam. It was necessary to fill the sheathing with water to sink it into place. The sheathing was very sensitive to unbalanced water levels. The sheathing would crush from excessive water on the outside or burst from excessive pressure on the inside. Numerous sheaths collapsed during the grouting states so this was abandoned in favor of inserting the tendon in the un-grouted sheath and simultaneously grouting inside and outside the sheathing in 10 foot lifts.

The test anchor program and the development of special construction requirements were instrumental in designing and constructing the 68 new post-tensioned anchors without a single failure. After almost a full year, the anchors were performing above the design expectations. The anchors proved to be a viable solution for the dam stability, without a significant change to the structural appearance. (Mortensen P.E., Boyd P.E., Vasquex P.E., Bruce Ph.D., & Carr P.E., 2012) Although this does not directly relate to the analysis of failure modes of tendons, it indicates the importance of quality assurance and using contractors with experience for this type of work.

The previous examples illustrate some data on the behavior, but mostly related to static conditions. There are no recorded failures of a PTA dam caused by a seismic event. Also, because of scale and similitude issues, there are not any physical tests or scaled model tests that

could be used as a basis to describe the events leading to failure. In the current literature, there is no sufficient information on how to evaluate tendons for failure mechanisms during a seismic event. Bond strength, creep and constructability are well understood. It is reasonable to assume if the PTA tendons fail, there is a high likelihood the section will fail. This thesis identifies the most likely modes of PTA tendon failure. A model with PTAs will be developed and subjected to seismic loads to develop a methodology to evaluate the likelihood of failure of tendons in both tension and shear.

### CHAPTER 3 : THE GENERAL DAM

In this chapter the parameter assumptions associated with the geometrical and material properties are discussed, as well as the types of loading and methods of analysis to evaluate the structural stability for concrete gravity dams. This provides the necessary background for the work completed in this thesis.

The model dam used for this thesis is based on an existing dam in Texas, constructed between 1911 and 1913. This structure is a concrete gravity dam consisting of three distinct sections with a crest length of 1580 feet; main dam section and two abutment sections. The main section of the dam, used as the model section for this thesis, has a crest length of 390 feet and a maximum structural height of 166 feet.

The typical cross-section of the dam consists of a vertical upstream face, 25 foot thick crest, and varying sloped downstream face. For this evaluation the downstream face of the dam was simplified with the following configuration; the downstream face is vertical from the crest to El. 1055.2, then slopes at 0.417 horizontal (H) to 1 vertical (V) (0.417H: 1V) to El. 1021.5, 0.607H: 1V to El. 982.2, 0.875H: 1V to El. 953.5, 1.03H: 1V to El. 913.1, then vertical to the base. The dimensioned cross section is shown in Figure 3-1.

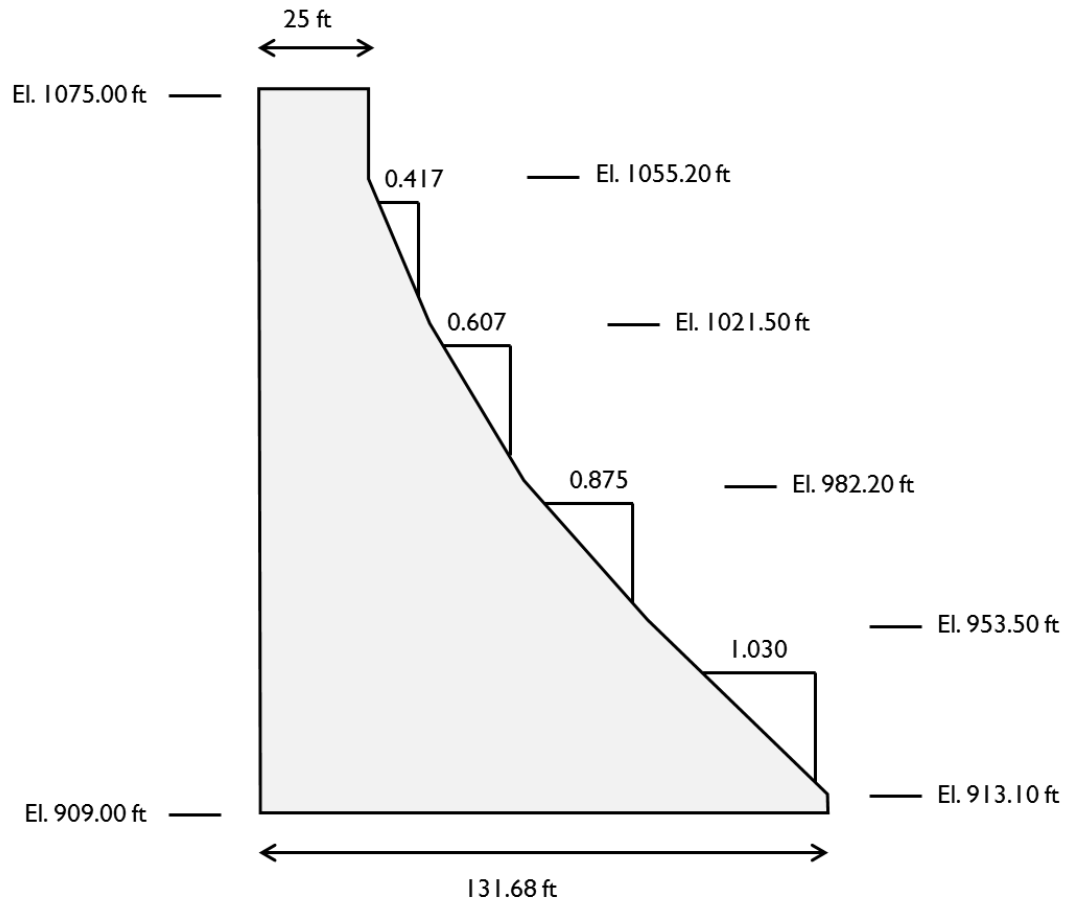


**Figure 3-1 General Dam Cross Section**

This dam was selected as the model for a number of reasons. The construction of the dam was completed over 100 years ago, and did not incorporate the effects of uplift pressure beneath the structure. The design flood has increased due to current understanding of the local hydrology, and the peak reservoir due to the design flood would be expected to overtop the crest of the dam. Therefore, this dam was found to have inadequate safety, and require post-tensioned anchors. The anchors were designed for maximum flood loading conditions.

The current understanding of seismic hazards has increased the expected design earthquake loads for dams throughout the country. While this dam in Texas is not in an active seismic area, it could represent other projects where a PTA design was performed for flood loads, only later to find that the seismic loads have increased.

The geometrical layout of the dam was a factor in selecting this project for this thesis. The height of the dam is a key characteristic in the behavior during a seismic event. This model dam has a structural height of 166 feet, and would develop greater oscillations during the seismic event, than compared to a dam with a height of 50 feet (considered a “small” dam).

Although this dam provides a great base for analysis, Texas is not a seismically active area. Since the Texas seismic loads would not induce enough excitement of the dam for proper analysis, seismic loads from a recently completed seismic study of the mid-Columbia region in Washington were used (URS Corp, 2012). Since Washington is a known active seismic zone, this data, which includes the response spectrum and acceleration time history record, were determined to have sufficient magnitude to evaluate the dynamic behavior of the dam (i.e. the loads would be large enough to excite the dam). Therefore, this thesis is the evaluation of the post-tension anchors during a seismic event, so a hypothetical project was appropriate.

### **Concrete Properties**

A gravity dam is constructed of mass concrete, which does not contain any reinforcement. The concrete strength is characterized by its tested unconfined compressive strength. An important characteristic of mass concrete is that the strength increases with the age of the material. Studies have shown that the strength gain can be as much as 20-50% in 5 years after the concrete was placed (U.S. Department of Interior, Bureau of Reclamation, 1977). Typically, the tensile strength of the concrete is approximately 10% of the compressive strength, which results in an approximate 10:1 compression: tension ratio (U.S. Department of the Interior, Bureau of Reclamation, 1987).

The elastic modulus of the dam is depended on the compressive strength. The compressive strength of the concrete is dependent on the rate of loading. The instantaneous

modulus of elasticity is usually assumed to be equal to the laboratory tested value of Young's Modulus. The rate of loading used in testing more closely simulates the high rate of load that corresponds to a dynamic event. Therefore, the laboratory value for the modulus of elasticity is used for dynamic load evaluations, and the static modulus is assumed to be about 67% of the instantaneous value (URS Corp, 2004).

The unconfined compressive strength has been shown to be 150% of the static strength for loads such as seismic events. Therefore, the sustained modulus of elasticity is used to simulate the behavior of the concrete during static loading conditions, and taken as 60-70% of the dynamic modulus of elasticity (U.S. Department of the Interior, Bureau of Reclamation, 1987). An example of the measured sustained modulus of elasticity and instantaneous modulus of Canyon Ferry Dam is shown in Figure 3-2.

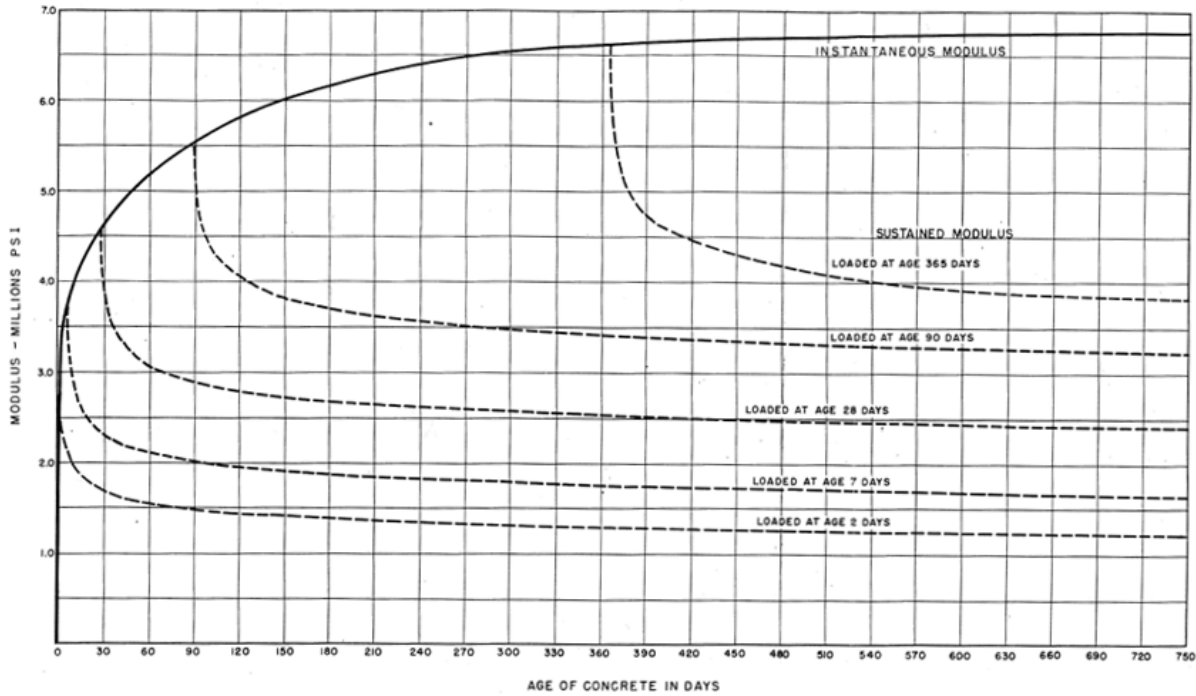


**Figure 3-2 Instantaneous and Sustained Modulus of Elasticity of Concrete – Canyon Ferry Dam (U.S. Department of the Interior, Bureau of Reclamation, 1958)**

As shown in Figure 3-2 (and is typical of concrete dams), the sustained modulus of elasticity continues to increase over time as the concrete strength continues to increase. The instantaneous modulus of elasticity remains higher than all measured sustained values. The average properties to use (in the absence of test data) according to the United States Bureau of Reclamation (USBR) are summarized in Table 3-1.

**Table 3-1 Summary of Average Concrete Properties from the Design of Small Dams (U.S. Department of the Interior, Bureau of Reclamation, 1987)**

<b>Property</b>	<b>Value</b>
Compressive Strength	3,000 to 5,000 psi
Tensile Strength (static)	5 to 10 percent of compressive strength psi
Tensile Strength (dynamic)	10 percent of static compressive strength psi
Shear Strength (static) Cohesion	10 percent of static compressive strength psi
Coefficient of Internal Friction	1
Poisson's Ratio	0.2
Modulus of Elasticity	
Dynamic Modulus of Elasticity	5,000,000 psi
Sustained Modulus of Elasticity	3,000,000 psi
Coefficient of Thermal Expansion	5.00E-06 ft/ft/°F
Unit Weight	150 pcf

Because test data is available for the general dam section (URS Corp, 2004), the concrete properties used for analysis are found in Table 3-2.

**Table 3-2 General Dam Concrete Properties (URS Corp, 2004)**

<b>Property</b>	<b>Value</b>
Compressive Strength	3774 psi
Tensile Strength	410 psi
Shear Strength	410 psi
Coefficient of Internal Friction	1
Poisson's Ratio	0.2
Instantaneous Modulus of Elasticity	1,700,000 psi
Sustained Modulus of Elasticity	1,200,000 psi
Unit Weight	136 pcf

Both the instantaneous and sustained modulus of elasticity values fall below the USBR values in the previous table. The USBR values are based on modern concrete mix design, and the model dam predates that technology. The lower elastic modulus values are probably related to the method used to place the concrete, water-cement ratios, mix design, cement type, and other factors.

## Foundation Properties

According to available information of the dam, the foundation rock is characterized as hard limestone (URS Corp, 2004). Typical construction techniques of the era in which this dam was built would have removed all deteriorated rock before construction of the dam began; therefore, the foundation of the dam consists of good quality rock, and was confirmed by field investigation data. Since the methodology of evaluation was the focus of this thesis, a conservative estimate for an effective internal angle of friction equal to 45 degrees was used for these studies. It is important to note, that the effective internal angle of friction consists of the base angle of friction plus the added effects due to irregularities and waviness of the potential sliding planes, such as the dam/foundation interface. The added effect of the irregularities and waviness, call the roughness angle, is dependent on the normal confining pressure at the base of the dam. For concrete gravity dams, the confining pressure is typically significantly less than the strength of the rock, and thus, the added roughness angle can increase the effective friction angle significantly (Hoek, Practical Rock Engineering - Course Notes., 2007)

The foundation deformation modulus was assumed to be approximately 900,000 psi and the unit weight of the foundation was assumed to be 145 pcf. These values were based on data from field investigations. These values are summarized in Table 3-3.

<b>Property</b>	<b>Value</b>
Effective Internal Angle Friction	45 degrees
Deformation Modulus	900,000 psi
Unit Weight	145 pcf

## Forces on the Dam

The forces acting on a gravity dam include: dead weight due to gravity, hydrostatic pressure due to the reservoir and tailwater, temperatures, internal hydrostatic pressure (i.e. pore

pressure or uplift in the dam foundation), ice pressure, silt pressure, earthquake, and forces from gates or other appurtenant structures. The additional load due to the post-tension anchors was also included in these studies. The USBR states that forces should be resolved into components normal and parallel to the foundation or to potential failure planes having significant slope in computing sliding stability. The applicable loads to this thesis are described below.

### *Hydrostatic Pressure*

The headwater and tailwater loadings are determined from the hydrology, meteorology, and reservoir regulation studies. The hydrostatic pressure against the dam is a function of the water depth multiplied by the unit weight of water. The unit weight should be taken at 62.5 lb/ft<sup>3</sup> even though the weight varies slightly with temperature (U.S. Army Corps of Engineers, 1995). There can be several reservoir levels that are of concern in the design and analysis of a concrete gravity dam. For usual (normal) loads the reservoir is typically taken at the highest normal operating level. For unusual (flood) loads, the reservoir is taken as the maximum (peak) level during the inflow design flood event, and can be higher than the crest of the concrete dam. For the extreme (seismic) load the reservoir level is typically taken as the usual water level.

For the General Dam, the maximum normal water surface (NWS) was assumed equal to El. 1064.2 msl with a corresponding tailwater surface (TWS) at El. 918.4 msl. The inflow design flood, which is equal to the probable maximum flood (PMF) reservoir surface, was estimated to be at El. 1087.1 msl, which overtops the dam by 11.0 feet, and corresponds to a TWS El. of 979.4 msl.

### *Internal Hydrostatic Pressure (Uplift)*

The distribution of internal water pressure along a horizontal plane through the dam or its foundation is assumed to vary linearly from full reservoir pressure at the upstream face to zero or tailwater pressure at the downstream face in the absence of drains. Internal water pressure (uplift) effectively reduces the weight of the structure, which results in a reduced normal confining (compressive) stress along the horizontal plane. In the presence of drains (dam drains or foundation drains), the uplift is still considered to be linear however the pressure head is reduced at the location of the drain, computed by Equation 3-1.

$$D_{Hd} = (1 - e) * (R_{Hd} - T_{Hd}) + T_{Hd} \quad (3-1)$$

Where:

- $D_{Hd}$  = Pressure head at drains
- $R_{Hd}$  = Reservoir pressure head at upstream heel
- $T_{Hd}$  = Tailwater pressure head at downstream toe
- $e$  = Drain efficiency, 82 percent

If analysis shows there is potential separation between the horizontal plane (i.e. cracking would develop), uplift pressure is increased to full reservoir head within the crack length, then assumed to vary linearly from the full reservoir pressure at the crack tip to the reduced head at the foundation drain location, and then vary linearly to zero or the tailwater head at the downstream toe (FERC Guidelines & Federal Energy Regulatory Commission, 1999).

If the crack extends past the drain location, a full reservoir head is assumed in the cracked portion which then varies linearly to zero or the tailwater head at the downstream toe of the dam (FERC Guidelines & Federal Energy Regulatory Commission, 1999).

The modeled section has drains approximately 112 feet from the downstream toe that are estimated to be 82% effective. The drain gallery is at EL. 925 feet.

## *Earthquake*

Three levels of earthquake conditions should be considered, which include the operating basis earthquake (OBE), a 25 year event, design basis earthquake (DBE), a 200 year event, and the maximum credible earthquake (MCE), the earthquake due to a known fault that produces the most severe ground motion at the dam site (FERC Guidelines & Federal Energy Regulatory Commission, 1999) (U.S. Department of the Interior, Bureau of Reclamation, 1987). Earthquake loadings incorporate both horizontal and vertical components of motion. While earthquake accelerations might take place in any direction, the analysis should be performed for ground motions oriented in the most unfavorable direction, which is typically the upstream-downstream direction (U.S. Army Corps of Engineers, 1995).

The hydrodynamic interaction between the dam and the reservoir adds inertia to the dynamic behavior of the dam. This can be simulated using Westergaard's formula, which computes a parabolic curve used to estimate the added mass from the reservoir. Westergaard's equation used for this thesis is shown in Equation 3-2 and Equation 3-3 (U.S. Army Corps of Engineers, 1995).

$$P_{ew} = \frac{2}{3} C_e(\alpha)y(\sqrt{hy}) \quad (3-2)$$

Where:

- P<sub>ew</sub> = Additional total water load down to depth y
- C<sub>e</sub> = Factor depending principally on depth of water and the earthquake vibration period
- α = Seismic coefficient
- y = Vertical distance from the reservoir surface to the elevation in question
- h = Total height of reservoir

$$C_e = \frac{51}{\sqrt{1 - 0.72 \left( \frac{h}{1000t_e} \right)^2}} \quad (3-3)$$

Where:

$t_e$  = Period of vibration, typically taken as 1 second

Unlike the static loading conditions, the uplift pressure beneath the dam is assumed to remain constant during the seismic event. Therefore, cracking at the base does not change the uplift pressure load, whereas a cracked base for static load must assume an increase in uplift load. Without a change in the uplift pressure, crack propagation is not as much a concern for seismic load. Therefore, the portion of the dam/foundation interface that is shown to develop normal tensile stress is typically considered to be damaged during the seismic load, and would be assumed cracked for a static post-earthquake loading condition. The post-earthquake load then increases the uplift pressure beneath the dam to account for the cracked portion of the base. The stability of the structure is then evaluated for the post-earthquake loading conditions. Also, the potential cracked base condition will result in a small elongation of the tendon, which could increase the tendon load. However, the additional elongation required to exceed 90% GUTS is approximately 2.5. Deformation of this magnitude is considered highly unlikely because of to the cracked base.

### **Loading Combinations**

There are four main loading combinations to take into consideration. The USBR also mentions the need to be conscious of load combinations, such that the ice load and maximum flood would not occur at the same time, along with it being unlikely the PMF and MCE would occur at the same time.

### *Load Case I – Usual Load Combination*

The reservoir elevation is at normal height along with the appropriate dead loads, uplift, silt, and normal tailwater.

### *Load Case II – Unusual Load Combination*

The unusual load condition is the flood condition that results in the reservoir and tailwater elevations which produce the lowest factor of safety. Dead loads, uplift and silt are also applied in this load combination.

### *Load Case III – Extreme Load Combination*

The usual loading is applied, along with the effects of the MCE.

### *Load Case IV – Post-Earthquake*

If the reservoir were to crack during Load Case III, case IV would be used to determine if the crack would propagate when the usual load case is applied (FERC Guidelines & Federal Energy Regulatory Commission, 1999) (U.S. Department of the Interior, Bureau of Reclamation, 1987).

## **Methods of Analysis**

There are two methods of analysis which will be used in this thesis. The first is the gravity method of analysis which is generally sufficient for the analysis of most structures. The second method is Finite Element Modeling which is a more sophisticated method of analysis as it provides point wise estimates for displacement and stress.

### *Gravity Method of Analysis*

The gravity method assumes that the dam is a 2 dimensional rigid block and the stress distribution across a plane is assumed to be linear. The gravity analysis should be completed before proceeding on to more rigorous studies since it provides good estimates at low computational cost. In most cases, if gravity analysis indicates that the dam is stable, no further analysis is necessary. The drawback to the gravity method is that the analysis does not take into account dynamic behavior characteristics which can magnify the effects of earthquake ground motions in the upper section of the dam (FERC Guidelines & Federal Energy Regulatory Commission, 1999), hence there is a need for a more detailed and accurate representation of the dam.

### *Finite Element Modeling*

In most cases, the gravity analysis method discussed above will be sufficient for the determination of stability for static loads. The Finite Element Method (FEM) allows the actual dam geometry to be modeled and accounts for its interaction with the foundation. Finite element analysis allows modeling of both the dam and the foundation. In gravity analysis, the distribution of foundation shear stress is not specifically addressed. Finite element modeling can give some insight into the distribution of base contact stress. Two-dimensional finite element analysis is adaptable to gravity dam analysis when the assumption of plane strain is used. Whatever distribution of stress that results from a finite element analysis, it should be verified that global force and moment equilibrium are satisfied. In addition, the stress states in individual elements must be within the limits of the material strength. For example, if the analysis indicates tension at the dam/foundation interface, the analysis should be re-run with tensile elements eliminated from the stiffness matrix. Finite element modeling allows for better modeling of geometry,

discontinuities, and dynamic properties (FERC Guidelines & Federal Energy Regulatory Commission, 1999). Details of the finite element analysis are not included as part of this thesis since the methods used were standard. The specific finite element software and methodology are included in a later chapter.

## CHAPTER 4 : METHODS OF FAILURE

The failure of concrete dams is typically described by using potential failure modes. There are four components to a potential failure mode (PFM). The first component is the initiating event, and is usually the normal operating load, flood event, or seismic event. The second component includes the progression of steps that lead from the initiating event to failure. This could include cracking in the concrete, a snapped tendon, or a multitude of other mechanisms of failure. After the failure is initiated, the third component includes the possibility for intervention; is there anything that could be done to prevent the failure from progressing further? And finally the fourth component is failure. In the instance of a dam, a failure is considered an uncontrolled release of the reservoir. This thesis focuses on the progression modes of failure of the dam and anchors. This chapter identifies the failure modes of the dam and post-tension anchors and provides the necessary information to evaluate these modes.

### **The Potential Failure Modes of the Dam**

The structural stability of a dam is evaluated in accordance with accepted criteria for the evaluation of concrete gravity dams, as summarized and explained in further detail below:

- **Concrete Overstressing.** Compares the computed stresses with the allowable strength of the concrete to determine if the material will crack or crush.
- **Overtopping Stability.** The forces and moments acting on the dam are used to determine the location of the resultant force and whether or not the dam/foundation interface separates (cracks) under any loading conditions.
- **Sliding Stability.** Evaluates the sliding stability along the dam/foundation interface.

## *Concrete Overstressing*

The structural capacity of the material in the dam is evaluated by comparing the calculated stresses from a structural analysis to the allowable tensile and compressive strength of the concrete. The allowable strength of the concrete is based on the stress versus strain behavior characteristics for concrete. Concrete is not a linear material and the stress versus strain relationship can be characterized into the following four stages:

- Stage I. The deformations and strains in the material are small, and the material is considered to be linear elastic, that is, when the load is removed the material returns to the initial unstrained state.
- Stage II. There is some inelastic behavior. The load results in minor permanent deformations and strain in the material, and when the load is removed the material does not return to the initial unstrained state (this is called hysteresis).
- Stage III. There are large inelastic strains resulting in a noticeable change in deformation. In this stage there is probably stable crack growth in the concrete, meaning that cracks will form but not initiate failure.
- Stage IV. Also called the fracture stage. The deformations are large enough to produce unstable crack growth and the eventual failure of the material.

Traditionally, the design and analysis of mass concrete has limited the material behavior to Stage I for usual loads, the Stage II for unusual loads, and the Stage III for extreme loads. The following bullets summarize the methodology in the limit state of the material for the corresponding loads:

- Usual loads traditionally limit the concrete behavior to the elastic range of the material, or Stage I. Studies on mass concrete have shown the material behaves linearly to approximately 35 to 50 percent of the ultimate strength (American Concrete Institute, 2005). Therefore, the maximum allowable stress for linear behavior of concrete is typically the static strength divided by three (U.S. Department of Interior, Bureau of Reclamation, 1977).
- Unusual loads traditionally have limited the concrete behavior to Stage II, which is considered relatively linear with some possible permanent deformation (hysteresis). Studies have also shown that growth of internal microcracks commences in the concrete at loads greater than approximately 35 to 50 percent of the ultimate strength (American Concrete Institute, 2005). The microcracks may result in some minor permanent deformation of the concrete; therefore, unusual loads limit the maximum allowable stress to the static strength divided by two (U.S. Department of Interior, Bureau of Reclamation, 1977).
- Extreme loads have traditionally limited the concrete behavior to Stage III, which would include permanent deformation and damage to the concrete. However, the damage is limited so as not to result in failure. The dynamic tensile strength usually corresponds to 150 percent of the static tensile strength, and the dynamic compressive strength corresponds to 130 percent of the static compressive strength (Raphael, 1984).

The stresses along the horizontal plane, within the dam are computed using Equation 4-1 and the potential for cracking in the concrete is evaluated based on Equation 4-2.

$$\sigma = \frac{P}{A} \pm \frac{M_c * c}{I} \quad (4-1)$$

Where:

- $\sigma$  = Stress at face
- P = Vertical force (lbs)
- A = Area of base
- $M_c$  = Moment about base centroid
- c = Distance from face to centroid
- I = Moment of inertia

$$\frac{f_t}{S} \geq pwh + \sigma_t \quad (4-2)$$

Where:

- $f_t$  = Tensile strength of concrete
- S = Safety factor
- p = Reduction factor to account for drains (1.0 if drains are not present)
- w = Unit weight of water
- h = Depth below water surface
- $\sigma$  = Tensile stress at face (without effect of internal water pressure)

The U.S. Army Corps of Engineers (USACE) allowable limits for both compressive stress and tensile stress are shown in Table 4-1.

**Table 4-1 Allowable Concrete Compressive and Tensile Stress (U.S. Army Corps of Engineers, 1995)**

Load Case	Allowable Compressive Stress	Allowable Tensile Stress
Usual	$0.3 f_c'$	0
Unusual	$0.5 f_c'$	$0.3 f_c'^{2/3}$
Extreme	$0.9 f_c'$	$1.5 f_c'^{2/3}$

## *Moment Equilibrium*

For overturning stability the summation of all forces acting on the dam must equal zero, hence implying moment equilibrium about an axis perpendicular to the plane of the dam cross-section. In linear elastic finite element analyses the base of the dam is assumed to be homogeneous, and can generate both compressive and tensile stresses. However, the dam/foundation interface does not have the capacity to develop tensile stresses. If tensile stresses develop at the interface, or across a weak plane within the dam, then separation (i.e. cracking) may occur along with the loss of contact.

Traditionally, safety against overturning has been evaluated based on the stress distribution from the upstream heel to downstream toe of the section. If the resultant force for the section was shown to fall within the middle third of the base, then (based on a linear stress distribution) by definition the entire base would be in compression. Thus, the middle third principle became the method to evaluate safety against overturning for normal static loads. For more extreme loads, such as the probable maximum flood (PMF) and maximum credible earthquake, then limited cracking was allowed at the base of the dam. Typical criteria used by the USACE to evaluate overturning stability are summarized in Table 4-2.

**Table 4-2 Summary of Overturning Criteria Based on the U.S. Army Corp of Engineers (U.S. Army Corps of Engineers, 1995)**

<b>Load Case</b>	<b>Location of Resultant Force</b>	<b>Allowable Crack Length (percent of base length)</b>
Usual	Middle third of the base	0-percent
Unusual	Middle half of the base	25-percent
Extreme	Within limits of the base	--
Post-Earthquake	Within limits of the base	--

The problem with the middle third principle and the USACE criteria is that the stress distribution at the base of gravity dams is not linear, and does not hold to the beam theory linear

stress distribution assumption. Thus, more recent guidelines, such as those published by the Federal Energy Regulatory Commission (FERC), allow for separation at the dam/foundation interface. Moment equilibrium, or overturning, is satisfied if the results show that base separation will not continue to propagate with the inclusion of modifications to the uplift pressure beneath the dam and in the cracked portion (FERC Guidelines & Federal Energy Regulatory Commission, 1999).

*Sliding Stability*

Sliding stability is the measure of determining the resistance of the structure against sliding. The sliding factor of safety is the ratio of the actual frictional shear resistance to resistance necessary to achieve force equilibrium. One of the main causes of uncertainty in the analysis of gravity dam stability is the amount of cohesive bond present at the dam/foundation interface. The FERC recognizes that cohesive bond is present, but it is difficult to quantify through borings and testing. The values presented in Table 4-3 offer alternative safety factors that can be used if cohesion is not relied upon for stability, which is the assumption in this thesis (FERC Guidelines & Federal Energy Regulatory Commission, 1999).

**Table 4-3 Summary of Minimum Allowable Sliding Factors of Safety based on FERC Guidelines (No Cohesion Assumption) (FERC Guidelines & Federal Energy Regulatory Commission, 1999)**

Load Case	Minimum Sliding Factor of Safety Neglecting Foundation Cohesion
Usual	1.5
Unusual	1.3
Extreme	1.3
Post-Earthquake	1.3

Sliding stability factors for concrete gravity dams are computed using Equation 4-3 (U.S. Department of the Interior, Bureau of Reclamation, 1987).

$$Q = \frac{c * A + F_N * \tan(\phi_e)}{F_D} \quad (4-3)$$

Where:

- Q = Sliding factor of safety
- C = Effective foundation cohesion (assumed 0)
- A = Area of uncracked base
- tan( $\phi_e$ ) = Effective coefficient of friction
- F<sub>N</sub> = Normal force
- F<sub>D</sub> = Driving force

The USACE, FERC, and USBR are not in full agreement with regards to sliding stability for the extreme load case. While the USACE requires the sliding factor remain above 1.1, the USBR requires the sliding factor to remain above 1, and Newmark's displacement analysis is applied to determine acceptability of implied displacements under earthquake loading. In this thesis the sliding stability factor of safety was not calculated for the extreme load. The seismic load results in oscillations of the structure, which infers the load direction is changing over time. For seismic evaluation the stability is assessed using permanent deformation and potential damage at the interface. These concerns are then incorporated in the post-earthquake analysis (U.S. Department of the Interior, Bureau of Reclamation, 1987).

### **Post-Tension Anchor Failure Modes**

The design and analysis of anchors includes determination of the anchor loads, spacing, depth, and bonding. Safety factors are determined by consideration of the following failures; within the rock mass, between the rock and grout/anchor, between the grout and the tendon, and yield of the tendon or top anchorage (U.S. Army Corps of Engineers, 1994).

The potential failure modes of the anchors can be divided into three general categories; tensile capacity, shear capacity, and environmental factors. Environmental failure mechanisms

may develop if precautions are not taken to keep the anchors dry and protected from the elements. Non-galvanic corrosion can cause the anchors to snap and break. This has led to the current state-of-the-practice to encapsulate the PTA tendons and anchor head with either grease or grout, as to prevent non-galvanic corrosion due to moisture and weathering elements. Environmental failure mechanisms are a concern for anchors, but were considered beyond the scope of this thesis, because this thesis evaluates a method of analysis for failure modes, and corrosion reduced the load capacity. Thus this thesis has the potential to assess the environmental effects as well.

### *Tensile Failure*

There are two critical components in the design and analysis of post-tension anchors; the anchor capacity and the load demand. The capacity of the anchor is estimated based on the physical and material properties of the anchor system. For example, the tensile strength of the steel and the cross sectional area are used to compute the capacity of the tendon. Design estimates the load required to stabilize the concrete gravity dam for the assumed loading conditions.

The load demand due to external forces, such as the reservoir force, can change during the extreme loading, primarily due to the oscillation that develops during an earthquake. Ultimately, the demand-capacity ratio (DCR) is used to evaluate the safety of the post-tension anchor system. If the demand is greater than the capacity (i.e.  $DCR > 1$ ) then it is assumed that tensile failure will develop.

Anchor head failure, foundation cone failure, bond zone failure and tendon tensile failure are all related to a tensile load, and ultimately a tensile failure of the tendon.

## Anchor Head

There are several potential ways an anchor head can fail. The wedges that grip the cable at the anchor head can make a notch in one or more wires, which would cause stress concentration in the wire and a tensile break at high loads (Madrazo, 2011).

Tendon wire breakage can also develop due to improper installation of the anchor head assembly such that the anchor head is not normal to the anchor orientation. This can be a result if there are uneven shim heights underneath the head assembly. Additional causes of cable failure that have been identified include spalling and cracking of concrete beneath the anchor head base plate which could cause the anchor head to rotate in turn crimping the cable leading to snapping of the tendons, poorly drained top anchorage ledges which could allow development of corrosion, or reduced strength, absence of filler grease in various areas, corrosion of tendons and eventually wire breakage (U.S. Nuclear Regulatory Commission, 2014). The maximum capacity of the anchor head assembly is typically assumed to be approximately 95% GUTS. At this load, the wedges may slip and crimp the cable and cause wires to fail (VSL International LTD, 1996).

## Foundation Cone Failure

The total length of the post-tension anchor tendon for a concrete dam is calculated from the height of the structure, and the anchor depth into the foundation rock. The anchor depth must extend for enough length into the rock mass to assure there is enough rock mass to resist the anchor design load. The length of the tendon in the anchor depth zone must be below the identified critical failure surface, such as the dam/foundation interface.

The anchor depth zone terminates at the end of the anchor bond zone, which is the length required to bond the anchor cable to the grout and rock mass. The bond zone pulls on the rock mass and forms an inverted cone, with the apex of the cone formed by normal (i.e. 90-degree)

intersecting surfaces. The geometry of the cone is influenced by the design spacing, or layout, of the post-tension anchor tendons. For this thesis the post-tension anchor layout was assumed to be a single row of anchors in fractured rock. Typically, the effective weight of the rock wedge (cone) must be greater than the design load of the post-tension anchor. Although, the depth of anchorage required for a single anchor in competent rock mass containing few joints may be computed by considering the shear strength of the rock mobilized around the surface area of a right rock wedge (U.S. Army Corps of Engineers, 1994). This cone shape is shown in Figure 4-1.

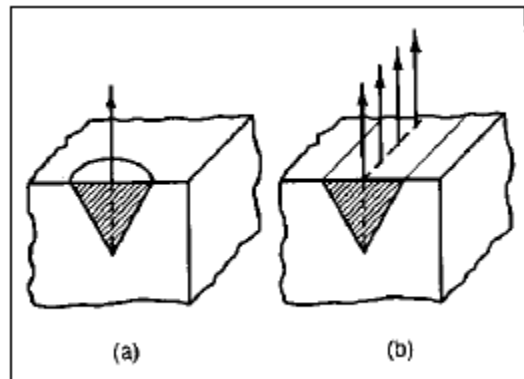


**Figure 4-1 Geometry of Rock Mass Assumed to be Mobilized at Failure (a) Individual Anchor in Isotropic Medium and (b) Line of Anchors in Isotropic Medium (U.S. Army Corps of Engineers, 1994)**

The equation to compute the depth of the anchor necessary to lie below the critical potential failure surface is shown in Equation 4-4 (U.S. Army Corps of Engineers, 1994).

$$D = \left( \frac{(FS)(F)}{\gamma S} \right)^{1/2} \quad (4-4)$$

Where:

- D = The required depth of anchorage
- FS = The appropriate factor of safety
- F = The anchor force required for stability
- $\gamma$  = Saturated unit weight of rock
- S = Spacing between anchors

A foundation cone failure is anticipated to occur when the factor of safety is equal to 1.

For this thesis, a factor of safety of 1 correlates to 118% GUTS.

### Anchor Bond Length

A post-tension anchor failure can develop with the bond between the cement grout and the side of the drill hole, or at the interface between the cable and the cement grout. The current design practice assumes there is a uniform bond distribution along the anchor length; however, this is seldom true in practice (Littlejohn & Bruce, 1975). As the load increases, progressive slip at the proximal end occurs. The location of the maximum intensity of bond stresses moves toward the distal end, which is shown in Equation 4-5.

$$\tau_x = \tau_0 e^{-\frac{Ax}{d}} \quad (4-5)$$

Where:

- $\tau_x$  = Bond stress at the distance x from the proximal end
- $\tau_0$  = Bond stress at the proximal end of the bar
- d = Diameter of bar
- A = A constant relating axial stress in the bar to bond stress in the anchor material

A is a constant with a theoretical trend relating the elastic modulus of the anchor to the elastic modulus of the rock material such that  $E_a/E_r$  is proportional to  $1/A$ . The larger the assumed value for the constant 'A', the greater the stress concentration at the free or proximal

end. The smaller the value for the constant 'A', the more evenly the stresses are distributed along the length of the anchor (Littlejohn & Bruce, 1975). Other influences on the bond failure include possible surface contamination of the bare strand bond length (i.e. grease from free length in bond zone), configuration of strands in the bond length (i.e. straight anchors versus anchors spirally rotated along the longitudinal axis), and drilling and flushing techniques (Klemenc & Logar, 2013). Local debonding at the strand/grout interface results in pullout of strands (Klemenc & Logar, 2013). Bond length failure was not considered as a variable in this thesis because the bond length is often determined by the contractor. Since the largest unknown when installing tendons is the strength of the bond zone, contractors will ordinarily add more tendon and increase the bond length, to reduce the risk of a bond length failure.

### Tendon Tensile Failure

A seismic event will oscillate the dam, which may cause elongation of the tendon and increase the load. The increase in the load on the tendon is estimated using Hooke's law, as shown in Equation 4-6. If the increased load demand on the tendon is less than the capacity of the tendon (i.e. DCR<1), then it is assumed that tensile failure will not develop.

$$P = \frac{AE\Delta L}{L} \quad (4-6)$$

Where:

- E = Elastic Modulus
- P = Axial load
- L = Length
- A = Area
- $\Delta L$  = axial deformation

It is important to note, that the capacity of the tendon can be affected by several outside influences. For example, corrosion can result in section loss, which then reduces the capacity, the

mechanical limitation of the anchor head, as previously described, typically is assumed to reduce the capacity of the anchor system to 95% GUTS. Movement in the foundation during a seismic event could result in damage to the bond at the cable/grout, or grout/rock interface, which may reduce the bond strength of the anchor system.

It is important that the effect of potential capacity reduction is evaluated in the design and analysis of post-tension anchors. The reduced load capacity can be simulated using hand calculations or a spreadsheet, and do not require complex numerical models. For example, if it is assumed that corrosion has reduced the section of the tendon that means there is less capacity, or less stabilizing force from the tendon. The results from the finite element model show the required load demand to maintain stability. The demand load can be compared with the estimated tendon capacity, with or without corrosion. If the analysis shows that the demand-capacity ratio is greater than unity, then it is reasonable to assume that the tendon has failed in tension.

If the load from the post-tension anchor is suddenly reduced, or lost due to failure, it can have drastic effects on the stability of a concrete dam. The loss of the tendon would likely occur during an extreme event, in which the load capacity of the tendon is required to satisfy moment and force equilibrium. If the tendon fails, there is a loss of equilibrium, which can result in catastrophic failure of the concrete dam.

### *Tendon Shear Failure*

When an earthquake event occurs of sufficient magnitude to develop oscillation of the structure, then there is a potential for horizontal displacement along a slip plane. If the horizontal displacement is large enough, it can result in shearing failure of the post-tension anchor at the sliding plane. Permanent deformation of the dam can be estimated using Newmark's method

(U.S. Army Corps of Engineers, 1999). This method as shown in Equation 4-7 determines the critical acceleration necessary to cause permanent deformation of the dam.

$$\frac{a_c}{g} = \frac{1}{(W+W_{a0})} [\mu_s(W - U) \pm H_s] \quad (4-7)$$

Where:

- $a_c$  = Critical acceleration
- $g$  = Gravity
- $W$  = Self-weight
- $W_{a0}$  = Hydrodynamic force
- $\mu_s$  = Coefficient of static friction
- $U$  = Uplift
- $H_s$  = Reservoir load
- $\pm$  = Sliding in upstream or downstream direction

Newmark's method computed critical acceleration for the structure, which is the acceleration that results in a sliding factor of safety equal to one (1). The process then evaluates the acceleration time history and compares it to the critical acceleration. Horizontal displacement is assumed to occur when the seismic acceleration is greater than the critical acceleration. The displacement is estimated using Equation 4-8.

$$s_m = \frac{v_m^2}{2a_c} \left(1 - \frac{a_c}{a_m}\right) \frac{a_m}{a_c} \quad (4-8)$$

Where:

- $s_m$  = Permanent displacement
- $v_m$  = Peak velocity
- $a_c$  = Critical Acceleration
- $a_m$  = Peak acceleration

The results from Newmark's method are used to evaluate the potential for a shear failure at the slip surface.

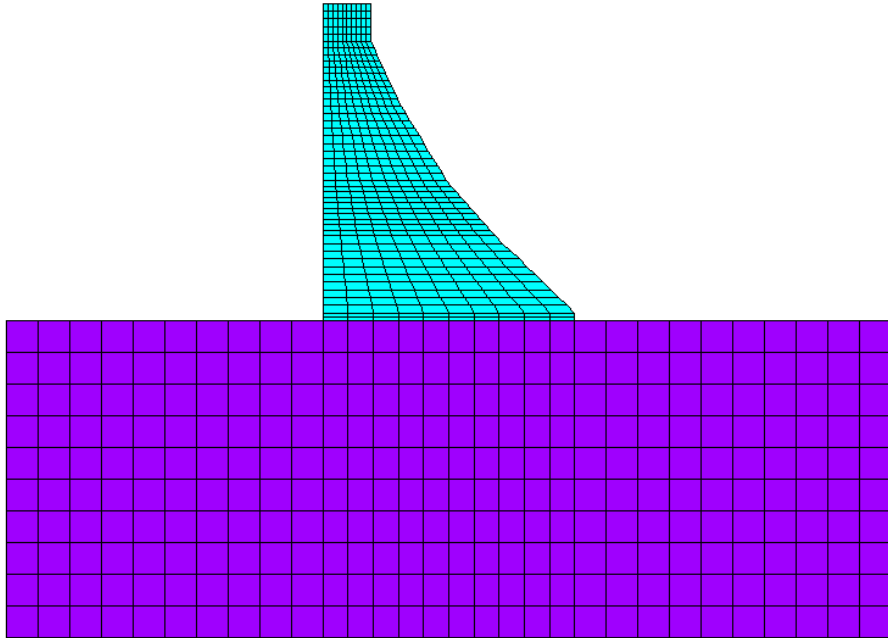
## CHAPTER 5 : ANALYSIS

This chapter describes the numerical model used to simulate the behavior of the concrete dam and post-tension anchors, and presents methods used to verify that the model is appropriately simulating the behavior of the structure and identifies the results that are of key interest in this work.

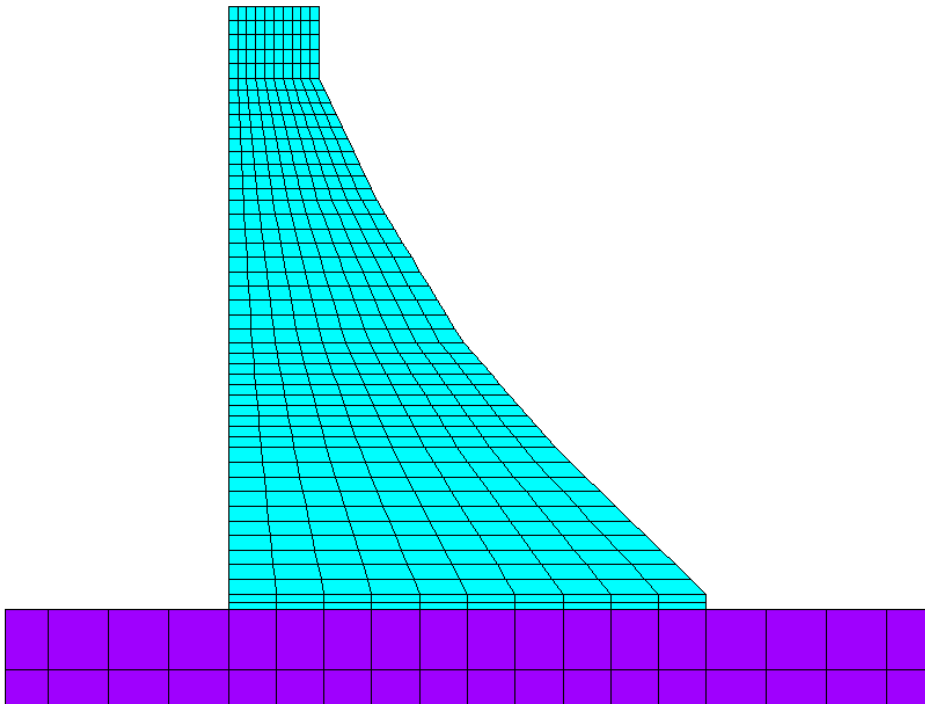
### **Modeling**

The cross section was simulated using a plane strain, two-dimensional (2D) finite element model, using ANSYS. The dam and a significant portion of the foundation rock were included in the finite element model. The geometry of the dam was based on the typical cross section as shown in Figure 3-1. The model includes a significant portion of the foundation extending approximately one dam height upstream, downstream, and below. The boundary conditions on the foundation are rollers; along the upstream and downstream edges the model is restrained against horizontal deformation, but free to move up and down, and the base is free to move horizontally, but restrained vertically. The concrete was modeled with the inelastic modulus of elasticity.

Both the dam and the foundation were modeled using 4 node brick elements, named plane182 elements in ANSYS (ANSYS, Inc., 2003). The full meshed model is shown in Figure 5-1A. Figure 5-1B is a zoomed in view of the meshed dam model with 903 elements and 970 nodes.



**A) Meshed Dam and Foundation**



**B) Meshed Dam Cross Section**

**Figure 5-1 Modeled Dam and Foundation**

## **Anchor Design**

The post-tension anchors were designed for the analysis in this thesis, based on the unusual (flood) load case, which includes the dead weight of the concrete, hydrostatic pressure to the peak reservoir level (El 1087.1. ft), tailwater, and uplift. The unusual load was found to be the controlling load case for the post-tension anchor design. Based on the results from the design calculations, the required anchor load was estimated to be 350 kips per linear foot of crest length.

The anchor layout consists of vertical anchors along the centerline of the crest, spaced at 10-foot centers. The post-tension anchor (PTA) consists of 53 0.6-inch-diameter, 7-wire strands with a yield strength of 270,000 lb/in<sup>2</sup>. The tendons were designed such that the working load (design load) is equal to 60 percent of gross ultimate tensile strength (GUTS), and the lock-off load was equal to 70 percent of GUTS. This provides 10 percent of GUTS for relaxation and creep of the tendon. The design length for the anchor is approximately 273 feet which includes 258 feet of free length and minimum 15 feet of bond length. The actual load due to the anchor design is approximately 3,540 kips per anchor, which is approximately 354 kips per linear foot of crest length.

## **Anchor Modeling**

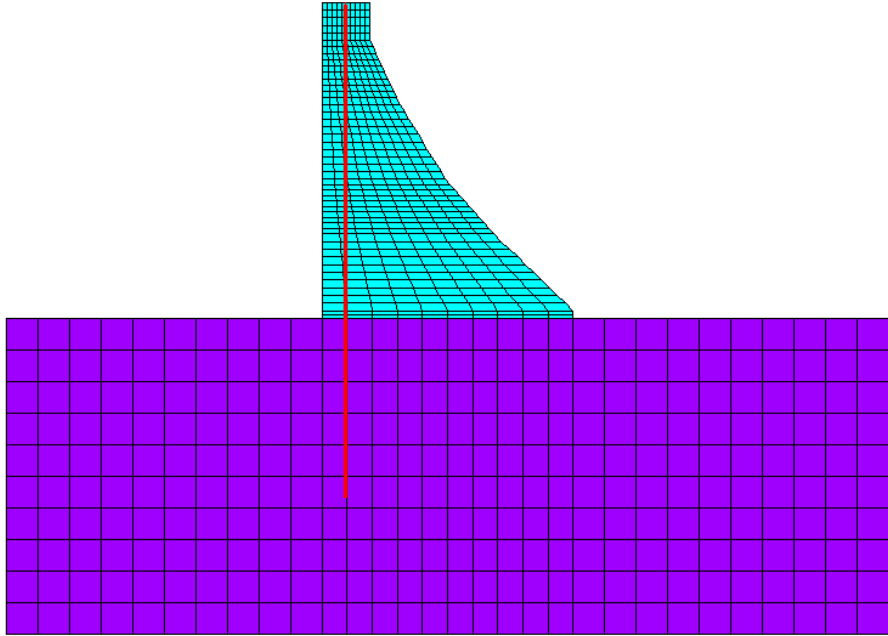
The anchors were first modeled as equal and opposite point loads at the nodes corresponding to the anchor location in the crest of the dam, and the top of the bond zone within the foundation. The advantage to using point loads is that it is a simple method to include the load on the finite element model. However, for dynamic loading conditions, the dam is oscillating, increasing the length of the tendon, which would change the applied load to the structure. The disadvantage to using a point load in the finite element model is that the load

remains constant during the seismic loads, and thus, may not be an accurate simulation of the actual behavior of the tendons and structural stability.

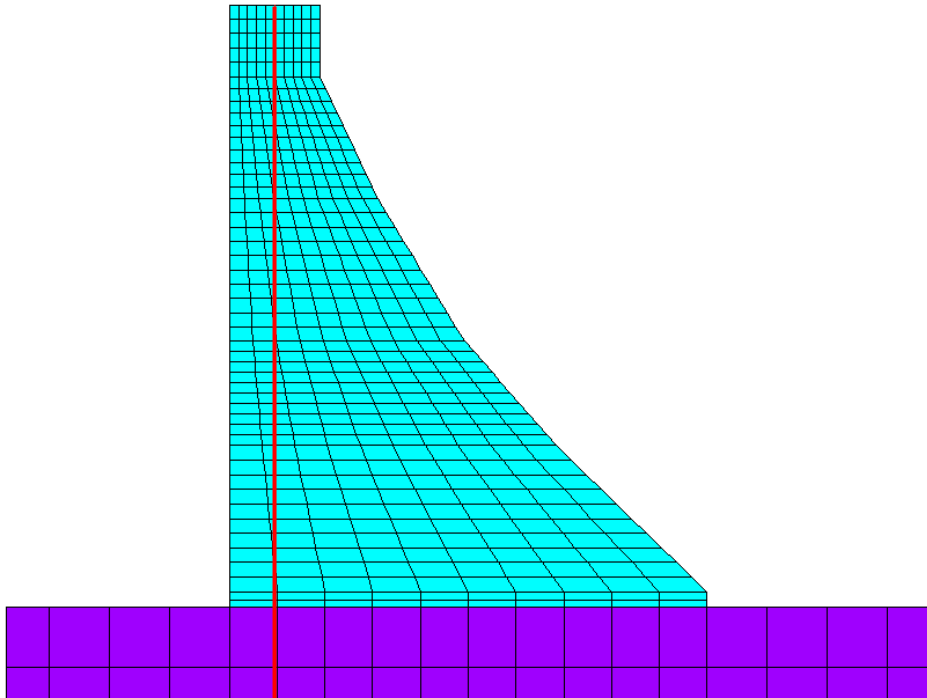
Another method to simulate post-tension anchors is to use a link type element, and set the initial condition of the link element to simulate the load from the tendons. This method was used for the final evaluations of the General Dam. The finite element model included a structural link element called a Link180 element in ANSYS (ANSYS, Inc., 2003). The end nodes for the link element were added to the model crest and foundation to simulate the location of the anchor head and bond zone. The end nodes for the link element were then coupled to the finite element model. The link element was inserted between the two nodes, shown in Figure 5-2.

Temperature stresses were applied to the link element to simulate the load on the PTA. A negative temperature load was applied to the link element, which resulted in contraction of the element and applied the load to the model. The applied temperature was determined through several sensitivity studies. The sensitivity studies applied various temperatures to the link element and measured the applied load from the results.

The results from the point load model, and the link model were compared to verify the load on the dam was behaving as expected. The results from the different models were used to plot the normal stress distribution at the dam/foundation interface. Based on the results, the link element model was considered to be the best representation of the post tension anchor load on the dam.



**A) Meshed Dam and Foundation with Tendon**



**B) Meshed Dam Cross Section with Tendon**

**Figure 5-2 Modeled Dam and Foundation with Link Element**

## Model Verification

Model verification was a multistage process, as shown below.

- **Static Load Case**

- The gravity method of analysis was used for the general section to compute the usual loads, which consists of the dead weight, normal reservoir level, tailwater, and uplift. The plots showing the stress distribution at selected elevations throughout the dam from the gravity method of analysis is shown in Figure 5-3.
- Analysis was also performed using the finite element method of analysis for the usual load case, and the stress distributions at the same elevations were plotted, as shown in Figure 5-4.
- Although the stresses are slightly higher at base in the finite element model, the overall results are trending in agreement and are what is to be expected. The sum of the forces and sum of the moments were checked against each other and showed less than a 5% difference.

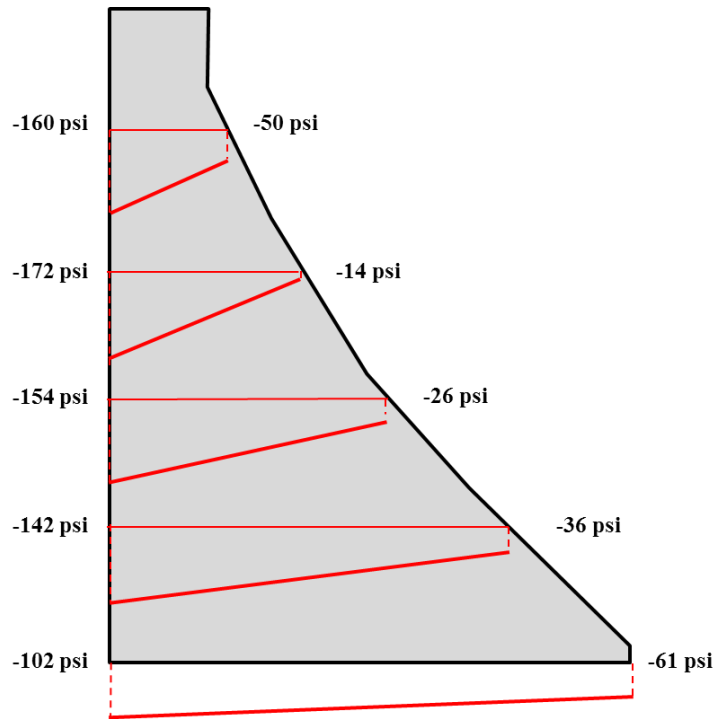


**Figure 5-3 Stress Plots of Static Analysis from Gravity Method of Analysis**

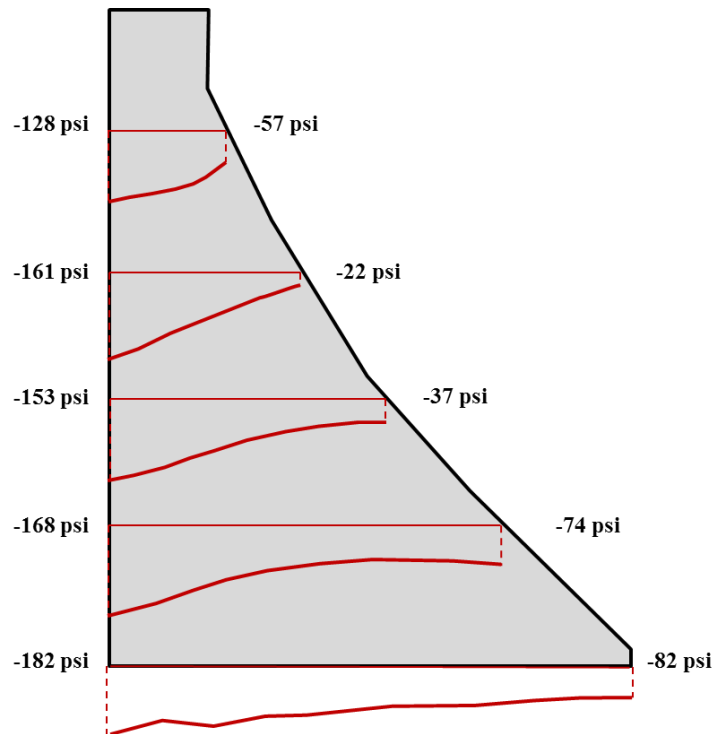


**Figure 5-4 Stress Plots of Static Analysis from Finite Element Analysis**

- **Hydrodynamic Load** – Westergaard’s added mass was computed by hand and then compared to the computed added mass at each node on the upstream face in the finite element model.
- **Modal Analysis** – Two methods were used to evaluate the fundamental modes of the dam. The first analysis used a simple approach developed by the University of California, Berkeley, and called Chopra’s method (Fenves & Chopra, 1986). The results from Chopra’s method were compared to the estimated modes from the finite element analysis. The peak ground acceleration (PGA) for the maximum credible earthquake (MCE) was assumed equal to 0.32g based on the results from the seismic hazard analysis. The resulting fundamental period for the structure using Chopra’s method of analysis was estimated to be 3.65/s. The fundamental period from ANSYS using the frequency and spectral values in Table 5-1 was 3.64/s, which is only a 0.3% difference. The first six mode shapes of the structure, with the PTAs are plotted in Figure 5-5.

**Table 5-1 Frequency and Spectral Values used for Response Spectra Analysis**

<b>Frequency (in/sec<sup>2</sup>)</b>	<b>Spectral Value (g)</b>
0.20	0.08
1.00	0.26
2.00	0.45
2.50	0.54
3.33	0.64
5.00	0.77
6.67	0.80
10.00	0.68
20.00	0.53
100.00	0.32

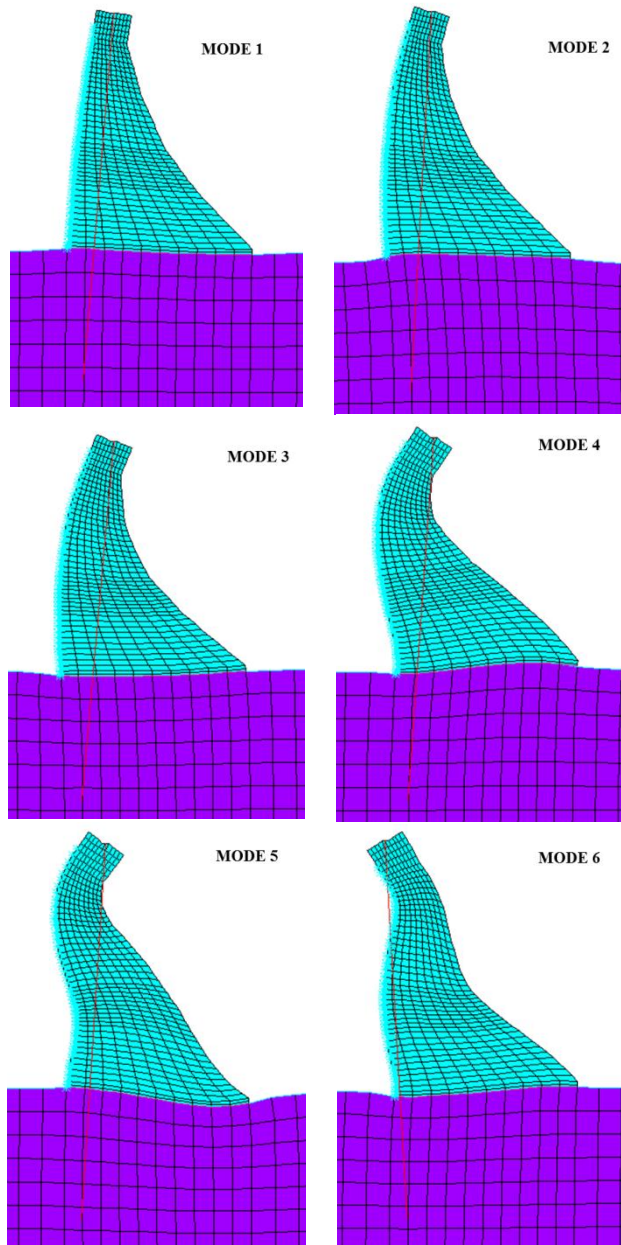


**Figure 5-5 First Six Mode Shapes with Post-Tension Anchors from ANSYS**

A pseudo-dynamic analysis, using Chopra's Simplified Analysis for Earthquake Resistant Design of Concrete Gravity Dams (Fenves & Chopra, 1986) was completed and the results were compared with the response spectra time history analyses using ANSYS. The response spectra analysis was run in ANSYS using the values shown in Table 5-1.

The stress distributions at selected elevations of the dam were computed using Chopra's method of analysis and are shown Figure 5-6. The stress distribution results from the finite element analysis response spectrum analysis are shown in Figure 5-7. Chopra's method of analysis is generally more conservative, which is shown by the larger values at the base of Figure 5-6. The sharp change in geometry above the top stress plot can help explain the difference in shape of the stresses (Chopra breaks the structure in to 10 blocks and averages geometries across those blocks). The comparison shows, since Chopra is generally more conservative, that there is a trend between the stress configurations.

The response spectra analysis adds the modal contributions together, which can be overly conservative. The actual behavior of the structure may see the modes cancel each other out. Therefore, it was considered important to perform a time history analysis to include the potential cancelling of the modes.

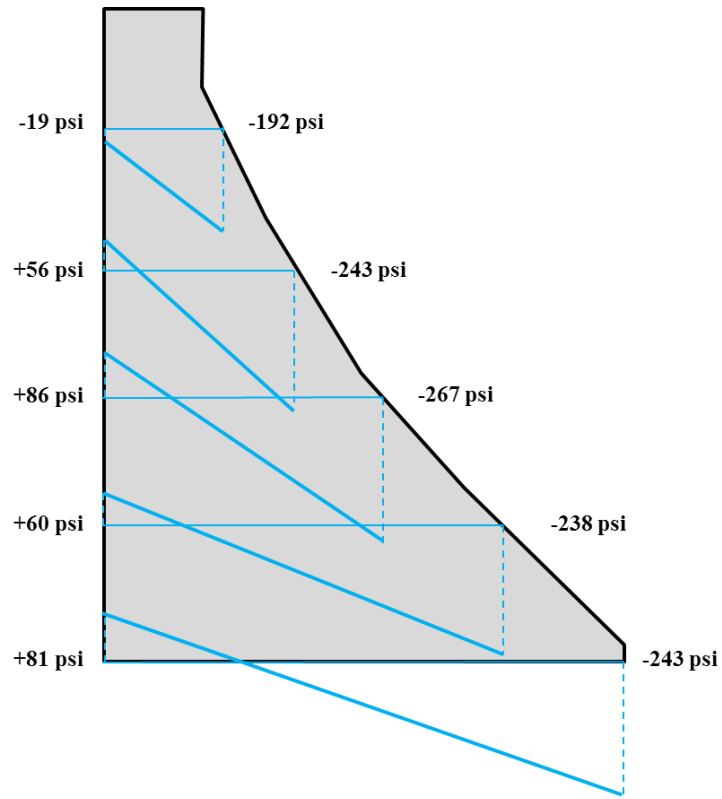


**Figure 5-6 Stress Plots of Pseudo Dynamic Hand Calculations**

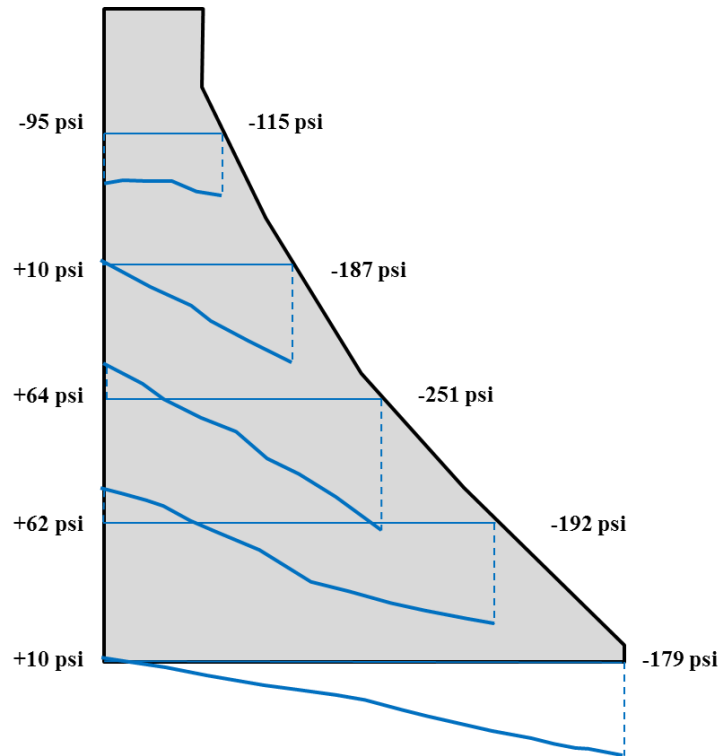


**Figure 5-7 Stress Plots of Site Specific Finite Element Analysis Response Spectra**

The time history analysis used the accelerations from the 1994 Northridge Earthquake, 1979 Imperial Valley Earthquake, and the 1971 San Fernando Earthquake. These root earthquake records from these events were spectrally scaled to match the target response spectra for the dam site. Two different dam target site spectrums were used, which resulted in six different time history events.

The finite element model was subjected to two components of acceleration, one horizontal and one vertical. The model was evaluated for a time step of 0.01 seconds to ensure that the responses from the contributing modes were fully captured. Although the recorded earthquakes extended for more than 30 seconds, the majority of the strong motion was complete after 15 seconds. Therefore, the dynamic behavior of the dam was only evaluated through approximately 15 seconds of the earthquake. The deformation results from analysis were used to evaluate at which time the most severe dynamic load develops on the dam. The controlling time history was found from the San Fernando record. The horizontal acceleration plot is shown in Figure 5-8.

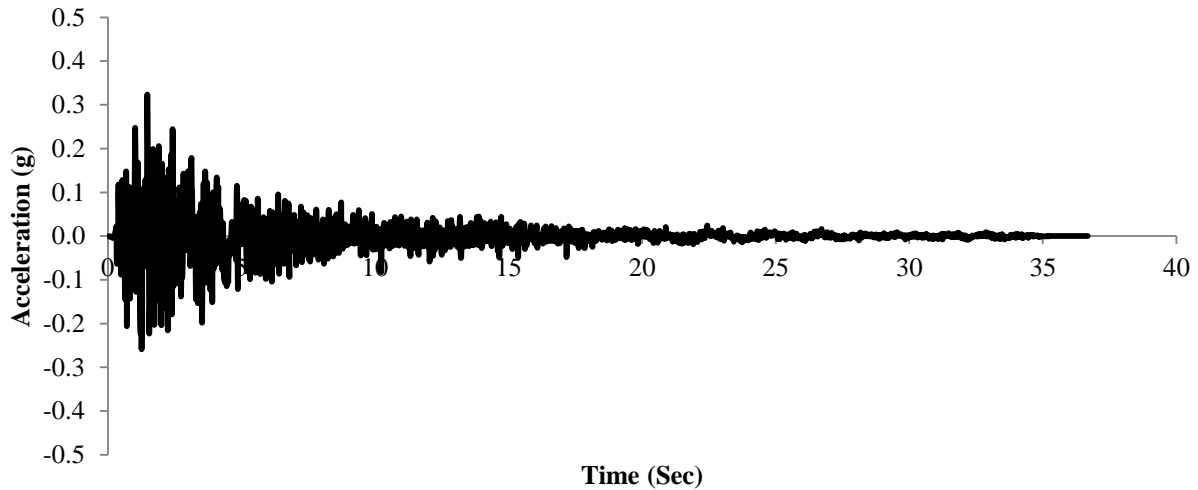


**Figure 5-8 Horizontal Time History of 10,000 Year Return Period for Controlling Seismic Event – San Fernando**

Once these time history analyses were completed, stresses were plotted at various elevations of the section for the time at which the most critical load developed on the model. The stress plots from each time history were compared to verify the stresses were trending the same. The stress distributions between the numerous stress plots were verified upon comparison. The stress plots from the time history analysis corresponding to the above response spectra table is shown in Figure 5-9. Because the loading varies between the response spectra analysis and time history analysis, general trends in the stress plots were checked.

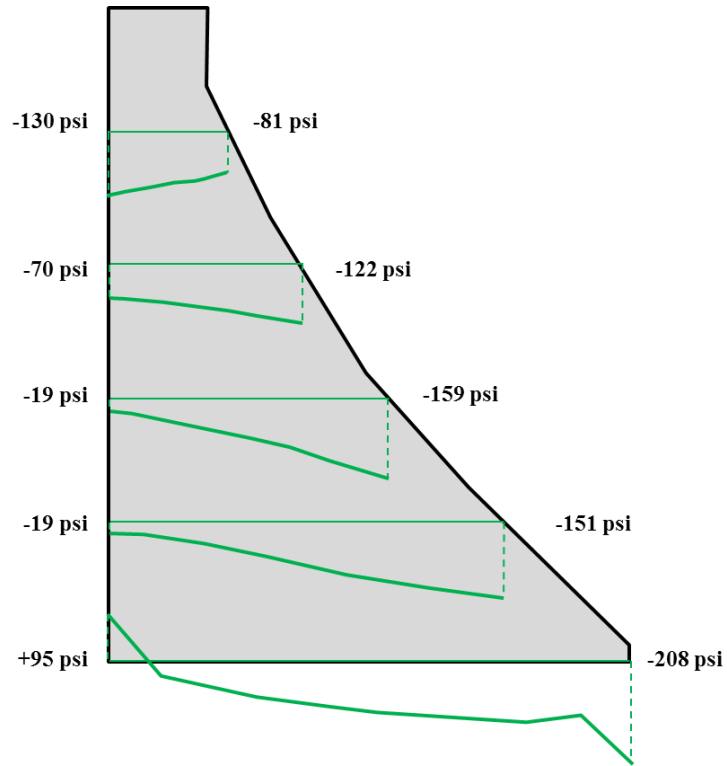


**Figure 5-9 Stress Plots of Spectrally Scaled Time History Analysis at Time 9.79 sec**

These verification steps verified the time history model, providing a basis to analyze the tendons for the various potential failure modes.

## CHAPTER 6 : RESULTS

This chapter presents the results from the completed analyses. As previously stated, there are a number of components that can cause failure of the post-tension anchor. Corrosion has proven to be a significant concern regarding the potential failure of anchors, however, for this thesis it is assumed that the anchor has adequate protection against corrosion, and that potential failure mechanism was evaluated. Similarly, the study has assumed that failure within the bond zone in the foundation would not occur.

### **Dam Failure Modes**

Initial studies found that the dam did not have adequate safety for the unusual load case without the post-tension anchors. Therefore, the post-tension anchors were designed for purposes of this thesis to ensure the safety of the dam against sliding and overturning. The resulting sliding stability factors of safety and location of the resultant force for the assumed loading conditions are tabulated in Table 6-1. These evaluations were a preliminary assessment of the dam safety, and used in the verification of static results from the numerical model. Although not tabulated, it is shown by the stress plots that the computed stresses in the dam are less than the allowable tensile and compression strength of the concrete. Therefore, the safety against overstressing of the concrete is considered adequate.

**Table 6-1 Preliminary Sliding Stability Factors and Resultant Location**

<b>Loading Condition</b>	<b>Sliding Stability</b>	<b>Resultant Location</b>	<b>Cracked Base</b>
Usual Condition	2.1	54.2%	0.0%
Unusual Condition	1.6	46.8%	0.0%
Pseudo static Analysis	*	30.3%	8.5%
Post-Earthquake Condition – 20% cracked	1.4	50.9%	20%

\*The sliding stability factor of safety was not calculated for the extreme load. The seismic load results in oscillations of the structure, which infers the load direction is changing over time. For seismic evaluation the stability is assessed using permanent deformation and potential damage at the interface. These concerns are then incorporated in the post-earthquake analysis. (FERC Guidelines & Federal Energy Regulatory Commission, 1999)

The plot of stress distributions for selected elevations is shown in Figure 6-1. The results indicate that a portion of the dam/foundation interface will separate (crack) due to the seismic loading condition. Based on the results, it is estimated that approximately 20% of the base length will crack and be subjected to the full reservoir pressure after the earthquake load. Therefore, for the post-earthquake load full uplift pressure was applied within the cracked portion of the base (20%). The results indicate that the crack would not continue to propagate, and would in fact close, showing the crack stabilized, which satisfied moment equilibrium. In addition, the results indicate the factor of safety against sliding is 1.4, which is greater than required in safety guidelines. The dam has adequate safety against overturning and sliding for the post-earthquake loading condition.

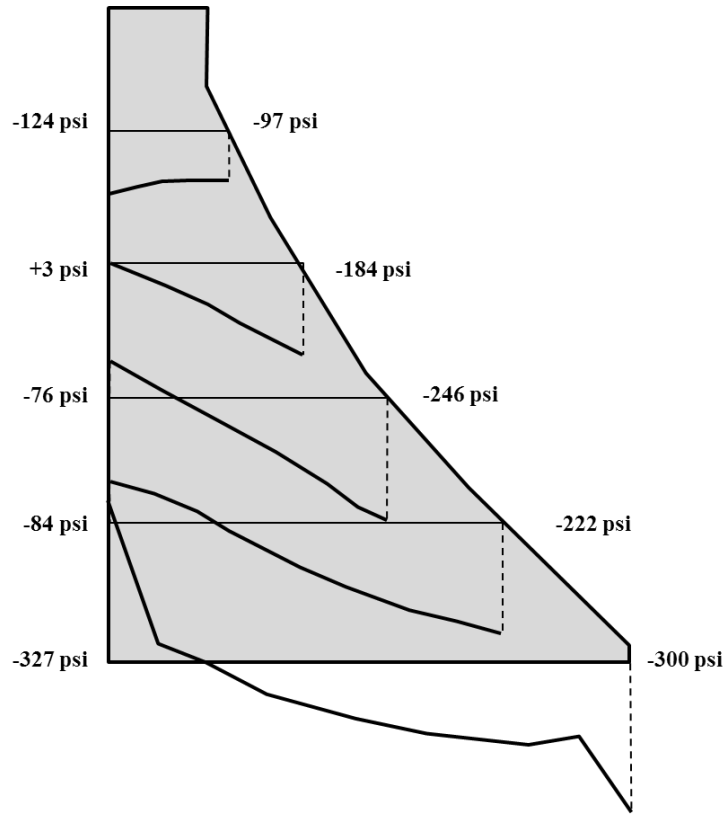


**Figure 6-1 Stress Plots of Governing Spectrally Scaled Time History Analysis at Time 1.61 sec**

### **Tendon Tensile Failure**

The horizontal and vertical deflection results were obtained from the finite element model at each time step of the time history analysis. The increase in the post-tension anchor tendon was computed using the increased elongation and Hooke's law. The results from the analysis are plotted as a percent of the gross ultimate tensile strength (GUTS) over the first 15 seconds in Figure 6-2.

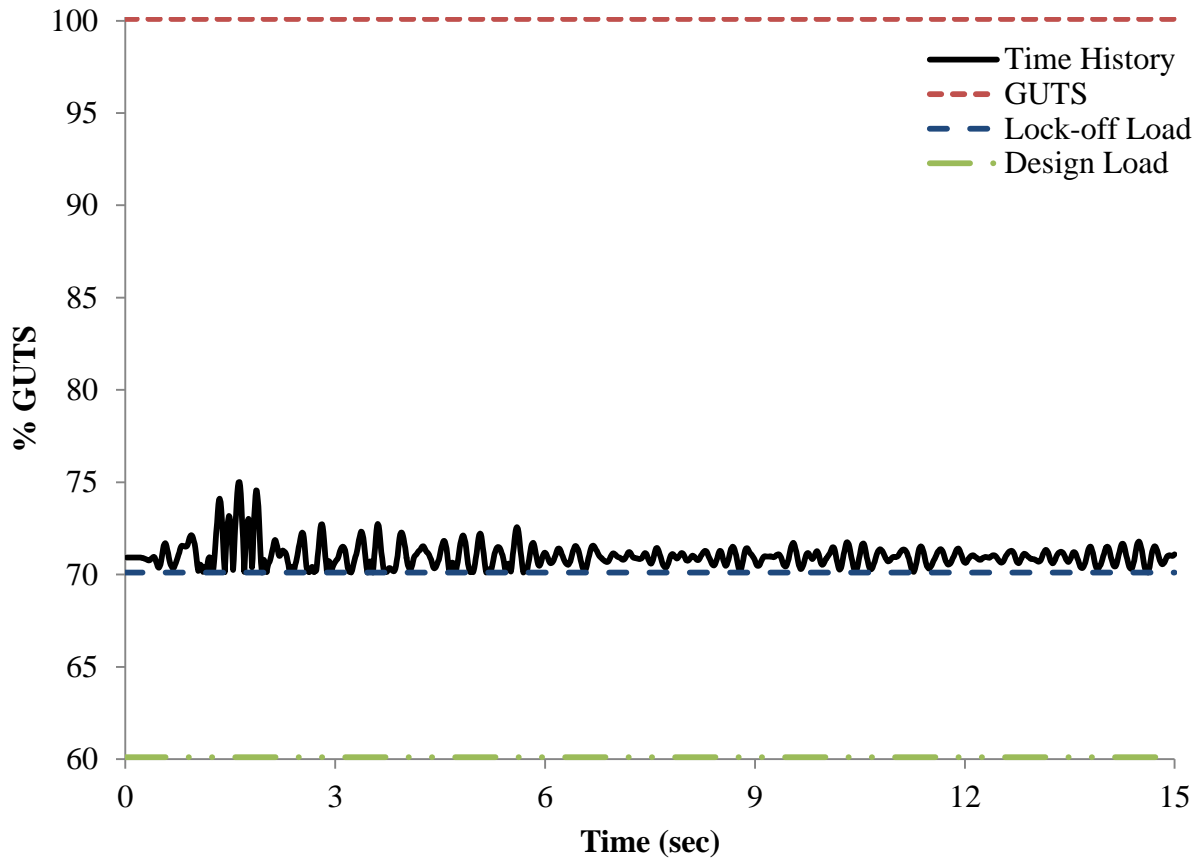


**Figure 6-2 Percent Gross Ultimate Tensile Strength of Post-Tension Anchor for Governing Time History**

The results indicate the potential increase in load on the post-tensioned anchors will not be greater than approximately 75% GUTS, or a demand to capacity ratio (DCR) of 0.75, which is significantly less than the capacity of the tendon.

As noted, the peak load on the post-tension anchor is approximately 75% GUTS. With a DCR of 0.79, the anchor is estimated to have adequate capacity. With a foundation cone failure expected at 118% GUTS, the foundation cone failure mode has a DCR of 0.632.

The results show this hypothetical project would have adequate safety against a tensile failure. The evaluation was successful in estimating the increase in the tendon load during the seismic event. The results can be used to assess the safety against various tensile failure mechanisms such as the tendon itself, the anchor head and foundation cone failure.

## **Tendon Shear Failure**

The results from the analysis were used to estimate the sliding stability of the dam during the seismic load. The results show there are periods of time at which the factor of safety against sliding is less than unity (1), thus indicating sliding will occur. Newmark's method was used in to evaluate the potential for sliding along the dam/foundation interface. Critical acceleration was estimated using the pseudo static analysis, and is considered conservative because it assumes a horizontal static load equal to the peak ground acceleration, whereas, the actual acceleration during the time history analysis will only be equal to the PGA for an instant, and less for the majority of the time. More importantly, the method can be incorporated with the results from the FEA model, by estimating the critical acceleration from the normal and driving loads from the FEA. Since the results indicated that the potential movement was not sufficient to develop a shear failure, no further study was considered necessary.

Newmark's method estimates the critical acceleration for the dam section, which was computed to be +/- 0.334g and -/+0.970g in the upstream and downstream directions. It is expected that the tendon would have a high probably of surviving the lateral displacement of approximately 0.33-inch along the base of the dam after the earthquake event.

The steel strands are stronger than the surrounding grout (i.e. tendon steel strength is 270 ksi and the grout strength may be between 4 and 10 ksi). If displacement were to develop, it is expected that the steel anchor would locally deform across the slip plane, and the steel would crush the grout and allow for the more ductile tendon to elongate within the smooth plastic sheaths. The diameter of the tendon cable is approximately 7 inches and the diameter of the hole is approximately 11 inches. Therefore, there will be close to 2 inches of grout around the tendon. This will allow for the crushing of the grout and deformation of the tendon.

This analysis shows that a potential shear failure of the tendons can be evaluated, even though this method uses several assumptions that have significant uncertainty. Changes in the foundation shear strength, reservoir interaction, and uplift assumptions all have an impact on the critical acceleration. If the critical acceleration and the seismic loading change, the results in turn also change. If the results show more shearing, then more study and physical tests would be necessary to justify if the tendon is adequate. Because of the number of assumptions used in Newmark's method, there is relatively low confidence in the results, and therefore shearing of the tendons must be included in a list of remaining concerns

All of these results must be viewed with one caveat in mind; there are no recorded seismic failures of this class of structure in the United States. Hence historical failures, and their sources, cannot be analyzed and compared with theoretical predictions. The combination of the physical dam and the imposed loads provide a representative scenario by which several of these failure modes could be explored, but these remain predictions until physical data can be procured.

## CHAPTER 7 : SUMMARY AND CONCLUSIONS

As gravity dams continue to age in the United States, it is becoming common to install post-tension anchors to enhance the strength of these structures for greater flooding and seismic events that are now considered possible. There is a lack of research and understanding as to how the anchors behave during a seismic event since there have not been any failures of this type. This thesis defined the potential failure modes associated with a representative post-tension anchored dam under common loading combinations. A finite element model was developed to evaluate the behavior of the tendons during a seismic event, and the results were used to evaluate the potential failure modes of the tendons:

- A literature review indicated there are three basic failure modes consisting of tensile failure, shear failure, and environmental failure. The primary failure modes that can be evaluated using numerical methods include tensile and shear failure.
- A method to evaluate failure of tendons during seismic loadings was developed. The methods used in the thesis were successfully able to evaluate the tensile and shear failure mechanisms.
- Although not the focus of this thesis, the results of the simulations indicated the dam had adequate safety against the PFMs. A sliding stability factor of 1.4 was computed for the post-seismic event, which included damage along 20% of the base that developed during the seismic event, which is higher than the minimum acceptable. Demand to capacity ratios (DCR) for the potential tensile failure modes were computed as 0.79 for the anchor head, 0.75 for the tendon, and 0.63 for the foundation cone failure.

- The results show the changing tension in the tendons can be determined from displacement results, and the potential for shear failure can be evaluated. The primary concern is shear, because of the number of uncertainties associated with the method.
- The uncertainties associated with many of the input variables associated with shear are important, and their influence should be evaluated further.
- Given the constraints associated with this study, it is anticipated that the most likely mode of failure for this class of structure would be shearing of the tendons, followed by a tensile failure. Of the three tensile failures presented in this thesis, the most likely failure would be at the anchor head, then tendon failure and finally a foundation cone failure.

Although not within the scope of this thesis, a pushover analysis would be the next step in understanding the failure of a post-tension anchored dam. A pushover analysis, or collapse mechanism analysis assesses the actual performance of the structure through a non-linear static procedure. The magnitude of loading or displacement is increased incrementally on the structure, until the structure is displaced or collapse would occur. This would incorporate the inelastic material response in the form of yielding of the tendons and cracking of the concrete. A pushover curve could be established and the weak links and failure modes would be found. (U.S. Army Corps of Engineers, 2007)

The possibility of shear failure developing in the tendons is of major concern. This thesis provides justification for the tendons not shearing in this hypothetical project; however the estimated displacement of the dam is relatively low. More research needs to be done to develop a better understanding of PTA shear failure, and the limits of dam movement. Future research

would include scale tests of the anchor at the dam/foundation interface and finite element modeling of the tendon-grout-foundation interaction along the base.

## BIBLIOGRAPHY

- American Concrete Institute. (2005). *Mass Concrete (ACI 207.1R-05)*.
- American Society of Civil Engineers. (2013). *2013 Report Card for America's Infrastructure*. Washington D.C.
- ANSYS, Inc. (2003). ANSYS User's Manual. Houston, Pennsylvania.
- Bruce, D. A., & Groneck, P.E., P. B. (1994). Dam Repair by Anchoring and Grouting: Some Recent Notable Case Histories. *USCOLD Dam Safety Modification and Rehabilitation*, (pp. 15-37). Phoenix.
- Fenves, G., & Chopra, A. K. (1986). *Simplified Analysis for Earthquake Resistant Design of Concrete Gravity Dams*. University of California, Berkeley, California: Report No. UCB/EERC-85/10.
- FERC Guidelines, & Federal Energy Regulatory Commission, D. o. (1999). *Engineering Guidelines for the Evaluation of Hydropower Projects*. Washington, D.C.
- Forbes, G., Wolfhope, P.E., J., Bruce, PhD., D., & Boyd, P.E., M. (2005). Post-Tensioned Rehabilitation of Hydropower Dams: Continuously Improving on an Anchor Program. *Waterpower XIV Conference*. Austin.
- Heslin, G., Bruce, D., Littlejohn, G., & Westover, T. (2009). Performance of Aging Post-Tensioned Rock Anchors in Dams. *ASDSO Northeast Regional Conference*. State College.
- Hoek, E. (2007). *Practical Rock Engineering - Course Notes*.
- Hoek, E., & Bray, J. W. (1981). *Rock Slope Engineering, Revised Third Edition*.
- Klemenc, I., & Logar, J. (2013). In-situ Tests of Permanent Prestressed Ground Anchors with Alternative Designs of Anchor Bond Length. *18th International Conference on Soil Mechanics and Geotechnical Engineering*, (pp. 2031-2034). Paris.
- Leamon, P. T., & Dunlap, P.E., L. F. (1994). Field Experience in the Behavior of Tendons Using Epoxy-Filled Strand. *USCOLD Dam Safety Modification and Rehabilitation*. Phoenix.
- Littlejohn, G. S., & Bruce, D. A. (1975). Rock Anchors - Design and Quality Control. *Sixteenth Symposium on Rock Mechanics*, (pp. 77-88). Minneapolis.
- Madrazo, G. (2011). *Post-Tensioning and Anchorage Systems*. NEES.

- Morin, P. B., Léger, P., & Tinawi, R. (2002). Seismic Behavior of Post-Tensioned Gravity Dams: Shake Table Experiments and Numerical Solutions. *Journal of Structural Engineering*, 140-152.
- Mortensen P.E., D., Boyd P.E., M. L., Vasquex P.E., V. M., Bruce Ph.D., D. A., & Carr P.E., P. (2012). Third Post-Tensioned Anchors Stabilization at Olmos Dam. *Association of State Dam Safety Officials Annual Convergence*. Denver.
- Mukherjee, B., Lague, G., Mosher, A., & Simon, Ph.D., P.E., A. I. (1999). Highgate Falls Dam Long Term Monitoring of Rock Anchors by Using Vibrating Wire Load Cells. *USCOLD Dealing with Aging Dams*, (pp. 111-129). Atlanta.
- Raphael, J. M. (1984, March/April). Tensile Strength of Concrete. *ACI Journal*.
- Tinawi, R., Léger, P., Leclerc, M., & Cipolla, G. (2000). Seismic Safety of Gravity Dams: From Shake Table Experiments to Numerical Analyses. *Journal of Structural Engineering*, 518-529.
- U.S. Army Corps of Engineers. (1994). Engineering and Design Rock Foundations. In *Engineering Manual 1110-1-2908*.
- U.S. Army Corps of Engineers. (1995). Gravity Dam Design. In *Engineering Manual 1110-2200*.
- U.S. Army Corps of Engineers. (1999). Engineering and Design Response Spectra and Seismic Analysis for Concrete Hydraulic Structures. In *Engineering Manual 1110-2-6050*.
- U.S. Army Corps of Engineers. (2007). Earthquake Design and Evaluation of Concrete Hydraulic Structures. In *Engineering Manual 1110-2-6053*.
- U.S. Army Corps of Engineers. (n.d.). *National Inventory of Dams*. Retrieved February 11, 2014, from <http://geo.usace.army.mil/pgis/f?p=397:5:525780895156001::NO>
- U.S. Department of Interior, Bureau of Reclamation. (1977). Engineering Monograph No. 19. *Design Criteria for Concrete Arch and Gravity Dams*.
- U.S. Department of the Interior, Bureau of Reclamation. (1958). *A Comparison of the Instantaneous and the Sustained Modulus of Elasticity of Concrete*. Denver.
- U.S. Department of the Interior, Bureau of Reclamation. (1987). *Design of Small Dams*. Denver: GPO.
- U.S. Department of the Interior, Water and Power Resources Service. (1981). *Water and power Resources Service Project Data*. Denver.
- U.S. Nuclear Regulatory Commission. (2014, February 11). *Information Notice N. 99-10*. Retrieved April 29, 2014, from U.S. Nuclear Regulatory Commission: [www.nrc.gov](http://www.nrc.gov)

URS Corp. (2004). *Lake Medina Dam Structural Stability Analysis*.

URS Corp. (2012). *Site-Specific Seismic Hazard Analyses for Lake Chelan, Rock Island, and Rocky Reach Dams, Central Washington*. Oakland.

VSL International LTD. (1996). *Detailing for Post-Tensioning*. Switzerland.

Walsh, K. Q., Draginis, R. L., Estes, R. M., & Kurama, Y. C. (2013). *Effects of Anchor Wedge Dimensional Parameters on Post-Tensioning Strand Performance*. Notre Dame: Report #NDSE-2013-02.

Zhang, H., & Ohmachi, T. (1999). Seismic Strengthening of Concrete Gravity Dams. *USCOLD Fifth Benchmark Workshop on Numerical Analysis of Dams*, (pp. 437-448). Denver.